Case Studies in Construction Materials 16 (2022) e01014

Contents lists available at ScienceDirect

Case Studies in Construction Materials

journal homepage: www.elsevier.com/locate/cscm

Molarity activity effect on mechanical and microstructure properties of geopolymer concrete: A review

Fatheali A. Shilar [a], Sharanabasava V. Ganachari [b,*], Veerabhadragouda B. Patil [c], T. M. Yunus Khan [d,e], Shaik Dawood Abdul Khadar [f]

[a] Department of Civil Engineering, Jain College of Engineering, Belagavi 590014, India
[b] Department of Chemistry, School of Advanced Sciences, KLE Technological University, Hubballi 580031, India
[c] Institute of Energetic Materials, Faculty of Chemical Technology, University of Pardubice, Studentská 95, 532 10 Pardubice, Czech Republic
[d] Research Center for Advanced Materials Science (RCAMS), King Khalid University, PO Box 9004, Abha 61413, Saudi Arabia
[e] Department of Mechanical Engineering, College of Engineering, King Khalid University, Abha 61421, Saudi Arabia
[f] Industrial Engineering Department, College of Engineering, King Khalid University, Abha, Saudi Arabia

ARTICLE INFO

Keywords:
Molarity
Activator
Alkaline to binder (A/B) ratio
Mechanical properties

ABSTRACT

The purpose of this paper is to discuss the effect of different molarity, Alkaline to Binder ratio (A/B), and Sodium silicate to sodium hydroxide (SS/SH) ratios on the enhancement of fresh and mechanical properties of geopolymer concrete. In addition, it also reveals the investigation of recent trends and technology of developments of geopolymer concrete in recent years. The fresh and hardened properties like, slump, compressive, split tensile and flexural strength, water absorption, and bulk density of geopolymer concrete data for molarity variations ranging from 5, 8–18 M, with A/B ratios ranging from 0.30 to 0.5, and SS/SH ratios. These data further assessed using kernel density plot. Molarity and A/B ratio maximum the strength development of geopolymer concrete is computed from the graph. The various binding materials used and tests performed on geopolymer concrete by the researchers are also highlighted in this paper. Increasing the molarity and A/B ratios results in the strength development of geopolymer concrete up to a specific limit.

Further increment of these parameters will not significantly affect the performance. The optimal value of molarity and A/B ratios at which give better performance is discussed in this paper. Structural performances of geopolymer concrete are higher than traditional concrete.

1. Introduction to geopolymer

Inorganic polymer concretes evolved as one of the novel alternative construction materials with the latent to custom a considerable component of sustainable construction material in recent years [1,2]. These materials are designed by the addition of alkali activation into industrial aluminosilicates waste materials like as fly ash (FA), ground granulated blast-furnaces slag (GGBS), metakaolin (MK), red mud (RM), etc. Geopolymer materials derivative from Si/Al-rich material reveal superior mechanical and chemical properties than conventional concrete [3,4]. Geopolymerization technology is the robustness and versatility of the production process. The chemistry of the geopolymer binder results in speedy strength development.

* Corresponding author.
E-mail address: sharanu14@gmail.com (S.V. Ganachari).

https://doi.org/10.1016/j.cscm.2022.e01014
Received 29 January 2022; Received in revised form 8 March 2022; Accepted 11 March 2022
Available online 12 March 2022

Nomenclature

A/B	Alkali/ Binder Ratio
Al	Alumina
M	Alkali Metal
ASTM	American Society for Testing and Materials
Al_2O_3	Aluminum Oxide
BK	Bulk Density
CA	Calcium
CASH	Calcium Alumina Silica Hydrate
C-S-H	Calcium-Silicate-Hydrate
CE	Carbon Emission
CS	Compressive Strength
$CaSO_4$	Calcium Sulphate
CTM	Compression Testing Machine
EE	Embodied Energy
FA	Fly Ash
Fe_2O_3	Ferric Oxide
GGBS	Ground Granulated Blast-Furnace Slag
GPC	Geopolymer Concrete
GPM	Geopolymers mortar
IS	Indian Standard
ITZ	Interface Transition Zone
K	Potassium
Kg	kilogram
K_2SiO_3	Potassium Silicate
KOH	Potassium Hydroxide
MK	Metakaolin
MPa	Mega Pascal
MJ	Mega Joule
Na	Sodium
Na_2SiO_3	Sodium Silicate
NaOH	Sodium Hydroxide
Na_2SO_4	Sodium Sulphate
NASH	Sodium Alumina Silica Hydrate
NBO	Nonbridging Oxygen
O	Oxygen
PP	Polypropylene fiber
RHA	Rich Husk Ash
RM	Red Mud
Si	Silica
SiO_2	Silicon Oxide
SiO_4	Silicon Oxygen Tetrahedron
Std.dev	Standard Deviation
WA	Water Absorption
°C	Degree Celsius

Proto-zeolite behavior of the geopolymer binder results in encapsulates for radioactive waste, specific, cesium, and strontium, which are chemically and efficiently immobilized by the geopolymer matrix [5,6]. The similarity of the two cementitious gels formed during polymerization, such as N-A-S-H and, C-A-S-H has a significant consequence in polymer concrete [7,8]. The various research from the past has insight into the usage of synthetic gels. The pH and aqueous aluminate, have intensely impacted the C-S-H structure. Ca ions modify into N-A-S-H gels resulting in partial replacement of sodium with calcium to formations of (N, C)-A-S-H gels [6]. There is a significant impact caused during the polymer synthesis and while polymerization by alumina's kinetics and calcium [9,10]. The variation in silica concentration has little impact on the rate of silica dissipation in decisive polymer gel and its mechanisms. This happens mainly due to the effort related to the separation of silica in reaction kinetics within the boundaries of a binder and alkaline activation [11,12]. Alkali-activation of polymer concrete with aluminosilicates along alkaline hydroxide used in the preparation of synthesis of inorganic geopolymer binder results in outstanding physical and chemical properties. Aluminosilicates gel comprising a three-dimensional structure of SiO_4 and AlO_4 ions led to tetrahedral shared O atoms [13]. The negative charge in the framework of tetrahedral Al is balanced by alkali metal. This aluminosilicates gel is used as a binder with various aggregates, such as natural rock and

sand, producing concretes [9,14]. The materials ingredients are rich in Ca, which results from the growth of critical phase formation of calcium silicate hydrate (CSH) and aluminosilicates gels [15,16].

The correlation between zeolites and N-A-S-H gels has significant impact on polymerization. Zeolites are synthesized under high pH in the matrix, and they are more stable to higher pH. However, zeolites perform [17]. CaO/SiO_2 led to increased composition changes along the C-A-S-H comprising phase concerning CaO. The presence of Ca, ion alters the cation mechanism to contribute to (N, C)-A-S-H until Na was interchanged by Ca. The role of Ca in the synthesis of Si/Al is determined by the polarizing power of Ca ion comparative to the alkali such as Na and K [18]. FA particles are rich in Si and Al.

Silica dissolution rate is associated with the dissolution rate of alumina. Dissolution of these ions is not identical, but local structural degradation of the FA resulted from the proclamation of one of the constituents, which increased the substitution of the other [19]. Different sizes and shapes of the FA particles, presences have different morphological features in the matrix. The effect of the water-to-binder (wb) ratio on pore solution alkali content specifies no noteworthy change during the reaction. The low alkali content in the matrix revealed poor mechanical properties causing friable in concrete [20,21]. The quantity of dissolved silica in the activator led to a considerable effect on alkali residual in the pore space. Higher silicate in matrix causes a higher reaction rate and lesser residual alkali [22,23]. Silica dissolved by the activator gives greater strength. While polymerization, the activator encounters lesser silica content than required for reaction, leading to low intensities of residual alkali in the pore space [24]. The mechanistic difference between hydroxide and silica in geopolymer formation led to some level of transformations in which gel precipitation occurs, with hydroxide-activator gels formed mainly on FA particle surfaces. Hydroxide activator in association with FA led to the formation of gel which consists of globular units, colloidal-size, close bond composed at their surfaces. Gel acted to be homogenous at the surface of the FA in the interstitial space [25]. Studies have also reported on the effect of addition silica and alumina on intermolecular bond formations [26] and the effect of adding glass powder, which actively influences STS [26].

The effect of the molarity of the activator agent on the strength development of GPC was investigated by understanding the pattern of results that were collected from earlier literature. The various binder materials and activator agents which are used in the preparation of GPC were reviewed. The ratios such as A/B, SS/SH, and their role in the strength development of geopolymer has been presented in this paper.

2. Geopolymerization process

Geopolymer belong to the ancestry of inorganic polymers. The chemical composition of these materials is almost similar to zeolitic only change that can be observed at the micro-level is that the microstructure is amorphous rather than crystalline [28]. The polymerization process comprises a rapid reaction rate in the presence of activator agents on Si-Al minerals, leading to the 3D geopolymer chain and forming the Si-O-Al-O bond. The primary conception in the polymer is that when Si/Al-rich materials are mixed with activator agent results in the development of Si-O-Al-O bonds through the polymerization process [29]. This process implicates a substantially faster chemical reaction in the presence of an activator on Si-Al-rich minerals that causes a three-dimensional geopolymer chain along with a ring structure that involves the formation of the Si-O-Al-O framework [30]. GPC forms the poly-condensation from Si and Al along with high alkali content led to the development of strength [31]. GPC is amorphous same as synthetic zeolites, and similar chemical composition as that of zeolitic structure. Geopolymers comprise a geopolymer Si-O-Al framework, dissimilar from zeolites, with alternate Si-Al forming tetrahedral linked together in 3-D by connected by oxygen atoms [32,33]. Al has four coordinated concerning oxygen produces a negative disproportion and cations like Na^+ and K^+ is necessary to fasten the process of rate of geopolymerization [34]. When water is added to NaOH and KOH agents, which liquefies silica and reacts vigorously with additives, led to the formation of a geopolymer binder [35]. The presence of industrial waste with rich Si and Al increases the strength. A higher amount of FA, GGBS, RHS, Metakaolin(MK), etc., as binder leads to higher content of Si, Al, and CaO, and ions enhance the strength development. Fly ashes have a wide range of reactivity, which has been used as one of the components of the geopolymer compounds made from them. These ions lead to evolution of C-S-H matrix, enhancing tetra-coordinated in the interlayer spaces [36].

Polymers formation as the same path as that of zeolites, such as the formation of mobile precursors through the measure of hydroxide ions, even part orientation of outrider, and partial restructure of the alkali polyciliate [37]. The composition of the initial reaction of a binder is the significant difference between polymerization and zeolite. The higher Si/Al ratio in the matrix and a growth in network connectivity of geopolymer gel that is SiO_4 tetrahedral exchange by AlO_4 tetrahedral [38,39]. Silicate used in surplus related to the extent of sodium hydroxide during the polymerization reaction, a concentrated amount of Al ions are released and react with them to form the framework of Si—Al—Ai bond [40].

3. Geopolymer chemistry

Combining a reactive aluminosilicate precursor powder with a highly soluble alkaline solution, such as Na/K hydroxide or silicate, is the most common way to make geopolymers.[5,39]. Hardening occurs at room temperature or at mild temperatures below 100 C, depending on the reactivity of the initial components. The rate of geopolymerization in matrix that results in nanometric macromolecules with a three-dimensional matrix made up of tetrahedral SiO_4 and AlO_4 that are randomly connected by sharing all oxygen atoms [41]. The negative charge of the AlO_4 tetrahedron, which contains the four-coordinated trivalent ion Al^{3+}, is stabilised by alkali metal cations such as Na^+, K^+, and Ca^{2+}.

Poly (sialate) is a term coined by Davidovits to describe the geopolymer structures, with "sialates" standing for alkali silicon -oxo-aluminate [42]. When hardened and glazed at temperatures exceeding 500 C, the inorganic polymer structure is X-ray amorphous at ambient temperature. Poly(sialate) has the empirical formula $Mn(–(SiO_2)z–AlO_2)_n.zH_2O$, where M is a cation such as K^+, Na^+, or Ca^{2+},

where z is 1, 2, 3, or higher, and n is the degree of polymerization [43]. Si/Al atomic ratio in the molecular assembly, four basic units is formed from this formula: SiAl = 1 (sialate), SiAl = 2 (sialate-siloxo), SiAl = 3 (sialate-disiloxo), and Si/Al> 3 (sialate link). Fig. 1 shows the life cycle process of geopolymer [11,42].

4. Reaction mechanism

The alkaline solution in geopolymer synthesis is often a permutation of MOH (M = Na, K) and alkali metal (M). In industry, soluble silicates (water glass) are frequently produced by alkali fusion of sand with soda ash or potash at temperatures approximately 1300 C, by dissolving the alkali silicate glass in water earlier or later cooling [33,44,45]. The hydrothermal dissolution of a reactive silica source in an activator agent is another way of creating silicate solutions. In general, the SiO_2/M_2O weight ratio (M = Na, K) describes the chemical composition of soluble silicates. This SiO_2/Na_2O is relatively near the molar in sodium silicates, while it is significantly different in KOH [21,44].

However, Na_2SiO_3 and K_2SiO_3 solutions appear identical, the former is less costly and more widely utilized. K_2SiO_3 solutions have particular benefits in terms of their properties [44,45]. The viscosity of K_2SiO_3 solutions is ten times lower than that of Na_2SiO_3 solutions for a given SiO_2/M_2O ratio, which is advantageous for getting high workability with less solution [45,46]. Furthermore, K_2SiO_3 solutions are less prone to generate efflorescence or the creation of alkali carbonate deposits, which is a crucial concern with sodium-based geopolymers. Finally, K_2SiO_3-based materials have more incredible refractory characteristics [48].

Although the process of geopolymerization is not well understood, it is thought to entail three significant stages. In that first stage, the breakdown of aluminosilicate materials by the severance of covalent Si–O–Si and Al links, resulting in the creation of silicate and aluminate [49]. This process is triggered by the hydroxyl (-OH) groups, which make the Si–O–Si bond more brittle. At high pH, reactive aluminosilicates dissolve quickly. In the case of metakaolin, dissolution results in the creation of ortho-sialiate molecules ($(OH)_3Si$–O–$Al(OH)_3$-Na^+), the fundamental unit in geopolymerization [27,47,48]. In the second stage, condensation of Si and Al monomers to form a matrix, at this point NaOH is liberated and again undergoes reaction [50]. There is the coexistence of two types of matrix; firstly, an aluminum-rich gel yields the GPC matrix, and another gel yields crystalline zeolite phases [51–53]. In addition, the water that was supposedly absorbed during the first phase is released during this operation. Secondly, Polycondensation and structural restructuring of the matrix, resulting in a three-dimensional geopolymer aluminosilicate network [1,54–56].

5. Interfacial transition zone

The interfacial zone (ITZ) between paste and aggregate is widely known as the weakest link in conventional concrete, where microcracks typically appear first under stress. This zone must be investigated ever since it is known to have a diverse microstructure after the rest of the hardened phase [57]. The increased penetrability of ITZ allows external agents such as chlorides, oxygen, and sulfates to penetrate the concrete structure more easily. The ITZ of GPC, on the other hand, has been characterized as denser and less microstructurally different from the majority of the binder area [3,58]. The ITZ adds to the GGPC increased splitting tensile strength, bond strength, and durability. The binding ability of the gel with natural aggregates increased when the concentration of the activating

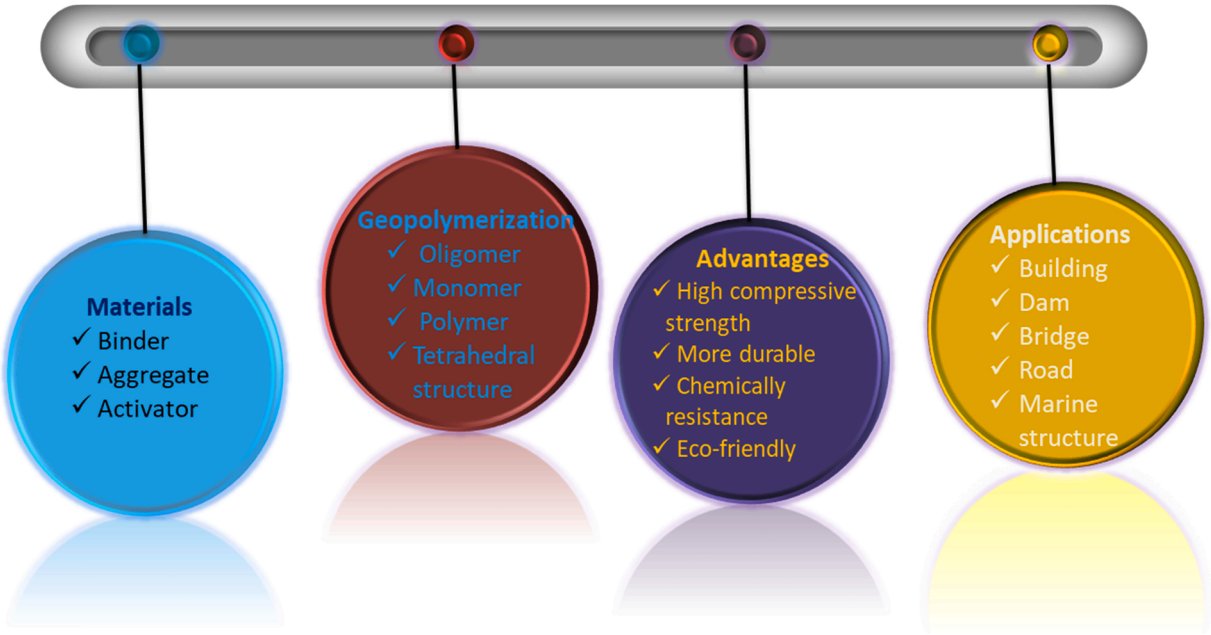

Fig. 1. Life cycle of geopolymer concrete.

solution was increased [31,59].

The addition of chloride reduced the interfacial bonding strength between the matix and aggregate, most likely due to crystallization of Si and Al. Researchers discovered that adding 0.5 M soluble silicate to an activating solution (10 M NaOH and 2.5 M Na_2SiO_3) enhances creating an aluminum-enriched aluminosilicate surface onto the aggregates by accelerating Si-preferential dissolution of kaolin and albite in another experiment [6,9,11,60]. The Si/Al ratio of the surface generated during albite leaching was identical to that of the real interface. There was no deposited aluminosilicate interface in the absence of soluble Si. This revealed that a full contact between silicious aggregates and geopolymer pastes requires both a high concentration of alkali and soluble silicate. There were several big voids in the fresh ITZ of potassium poly(sialate) geopolymer concrete. As the hydration process progressed, these voids were entirely filled with hydration products [13,61,62]. Low superplasticizer doses (3%) resulted in a loose and porous ITZ, whereas greater dosages resulted in a thick ITZ between the aggregate and matrix (7%). They also discovered that when the thickness of ITZ was reduced, the compressive strength increased and that this connection was dependent on the superplasticizer dose[63,64].

Si and Al are tetrahedral coordinated to oxygen, but additional bonds are not shown for clarity [16,60,61]. Atomic structure for the intermediate model, alongside purely crystalline and amorphous model with Si: Al molar is shown in Fig. 2(a). This graph depicts the overall oxide compositions, the amount of ash present, and the strength obtained by activating those ashes [66–68].

Na and Ca ions significantly more severe "damage" to the glass structure produced by removing a divalent cation than a monovalent one [18,62]. It has been hypothesized that the first phase of the mechanism of glass dissolving at relatively high pH parallels that found under acidic circumstances, with ion exchange of H for Na or Ca initiating the process. While it is difficult to see such a mechanism becoming significant at a pH close to 14, as is the case in the early stages of two-part (alkali-activated) geopolymer syntheses, it will

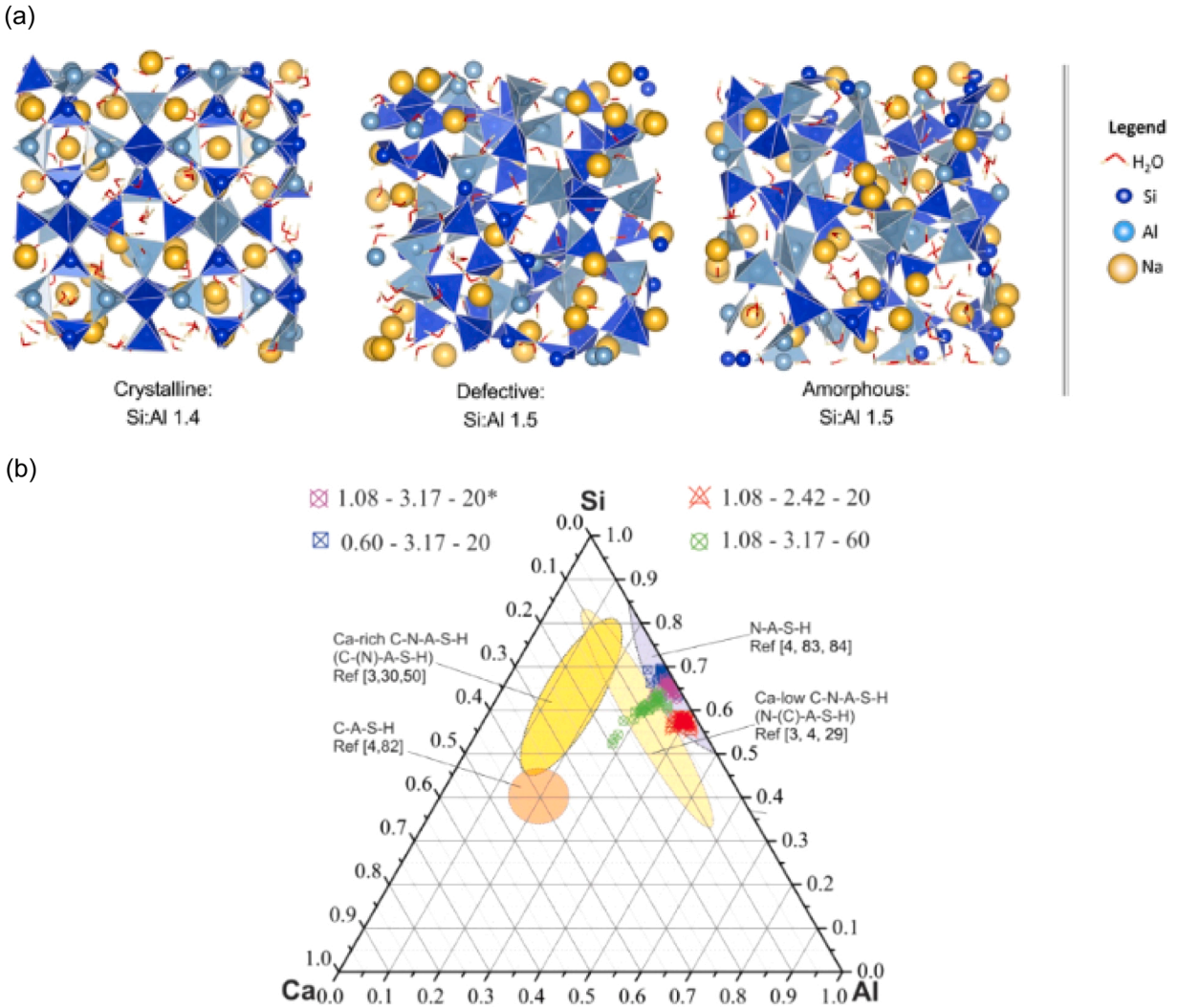

Fig. 2. (a). Atomic structure for the intermediate model, alongside purely crystalline and amorphous model with Si:Al molar. Fig. 2 (b). Ternary Diagram Al-Si-Ca of GPC showing the compositional range for C-(A)-S-H, C-N-A-S-H and N-A-S-H.
(a) [Figure is reused from reference [64]. (b) [Figure is reused with permission [69].

undoubtedly be conceivable early in the process [19,63]. While it is well known that surface-charging behavior governs the network breakdown process during glass dissolution. More straightforward situations (such as crystalline quartz dissolution) remain a source of debate. As a result, particle being bonded by water and hydroxide, although the precise sites at which each process occurs are not specified. Compositional Ternary Diagram Al-Si-Ca is represented as showed in Fig. 2b.

Similarly, some glasses exhibit simultaneous Si and Al release, whereas others selectively leach one component; this is mainly reliant on the specific glass employed, and the leaching environment and the specific specifics are extensively documented [46,64–66]. The presence of alkaline earth cations in a glass increases the likelihood of framework disorder, including producing a tiny concentration of (weak, reactive) Al–O–Al bonds and a nonbridging oxygen (NBO) content higher than stoichiometry requires. As a result, it's simple to see why slag, high in Ca^{2+} and Mg^{2+} as modifiers, is an ideal raw material for alkali activation [52].

6. Materials used as the binder and activators

The choice of the ingredients of materials for geopolymer concrete (GPC) helps develop better structural performances of GPC [70]. Numerous waste materials are generated from various industries or by-products such as FA, GGBS, red mud (RM), micro silica(MS), metakaolin MK, rice husk ash (RHA) used as the binder for the production of GPC composites. Table 1 represents the various binder materials, SS/SH, A/B ratio, and tests carried out by the various researchers. The primary source of these materials composition consists of substantial reactive Si and Al oxide, leading to a better polymerization rate. Composite binder FA-GGBS activators are reacted with aluminosilicates powder in the presence of Al_2O_3, dissolution of Si and Al ion releasing SiO_4, and AlO_4 into the solution during polymerization [37,71]. This results from the rapid rate of chemical reaction leading to the strength of the bond Si-O-Al-O; thus, further reaction led to the Polysialates framework. The reactivity of FA depends on various factors such as fineness, % of reactive silica, and quality of coal used for the preparation of fuel [38]. FA is spherical, and the specific surface is more excellent than Portland cement. FA particle size ranges from 1 to 150 μm. Class F, FA is the desired material for Class C to prepare concrete. The characteristics

Table 1
Represents various parameters considered for the preparation of GPC by various researchers.

Binder Used	Molar Concentration (M)	Na_2SiO_3/NaOH Ratio	Alkaline/Binder Ratio	Parameter Analyzed	References
FA+GGBS+ Glass Powder	4,8,12	–	0.31,0.33, 0.35	CS, STS, FS	[28]
FA+GGBS	8,10,12,14,16	0.5,1,1.5,2,2.5,3	0.25	CS, STS, FS, WA, BD	[78]
FA+GGBS+FIBRE	8,10,12,13,14,16, 18	–	0.61	W, CS, STS, SEM, EDS	[20]
FA+ Nano Silica	8,10,12	–	0.4	CS, STS, FS, WA, DB, RCPT	[71]
FA	12,16,18	0.4,0.5	0.3,0.35,0.40, 0.45	W, CS, STS, WA, MoE	[72]
FA	10,15,20	0.61,1,1.5,3	–	W, CS	[79]
FA+Bottom Ash	5,10,15	1.5	–	CS, FT-IR, DSC, SEM	[13]
FA	8,10,12,14,16	1.5,2.0,2.5	0.4,0.5,0.6	CS, FS, BD, WA, SEM	[46]
FA+GGBS	12,14	2.5,3.0,3.5	0.3,0.35,0.4	CS, STS, FS	[21]
FA	6,9,12	–	0.5	CS, SEM, EDS, XRD, FT-IR	[80]
FA+GGBS	14,16	1.5	0.5	W, CS, WB, FS, SEM, EDX	[10]
FA	8,10,12,14	2.5	0.45	W, CS	[37]
FA	5,8,12		0.3	CS, FTIR, SEM, XRD	[66]
FA+ GGBS+ Silica Fume	10,12,14,16	–	0.3,0.35,0.4,0.40.5	CS, FS, SEM	[26]
FA+ GGBS+ Waste Ceramic+ Waste Bottle Glass	2,4,6,8,10,12,16	3.0	0.55	Setting time, W, CS, STS, BD, SEM, XRD, FS	[14]
FA+ , GGBS + Silica +Red Mud	6,8,10,12,16	–	0.32	CS, BD, SEM, XRF, TEM, HRTEM, FTIR	[35]
FA+GGBS+Silica Fume + Nano Silica	12	2.0	0.45	CS, XRD, FTIR, SEM	[81]
FA+ MK	14,20	0.79,1.18,1.28, 2.0	0.26,0.28,0.31,0.33,0.39,0.43 0.50	W, CS, STS	[82]
FA+RHA+GGBS	12	–	0.47	W, CS, XRF, XRD, PSA, FTIR, FESEM	[9]
FA+GGBS+RHA	14	0.55	0.55	Chloride Permeability, Sorptivity,SEM, EDS, XRD	[83]
FA+ Nano SiO_2 + Nano $CaCO_3$	8,10,12	–	0.3	CS, FS, Flow test, FESEM, Ultrasonic pulse velocities	[84]
MK+ Waste Glass+ Nano Silica	10,20,30	1.50	0.82	Porosity, FS NMR	[85]
FA+Kaolin+OGPC	14	2.5	0.4	FTIR, Temperature and admixture effect on CS	[86]
GGBS+ Rubber	–	–	0.38	CS, STS, FS, Impact test	[87]
FA+ GGBS+ Kaolite	12	2.5	0.54	CS,FS,MoE,WB, Permeable	[88]
MK+Red Ceramic Waste	13	–	1.0	CS, XRD, FTIR, FESEM	[89]
FA+ Silica Fume	14	2.5	0.4	W, CS, STS, FS, SEM	[38]

W-Workability, CS-Compressive Strength, STS-Split Tensile Strength, FS-Flextural Strength,
WA-Water Absorption, MoE-Modulus of Elasticity,BD-Bulk Density,S-Sorptivity

of FA are more appropriate for the preparation of GPC [40]. Researchers have appealed that to produce binding properties using low-calcium FA with low CaO content less than 5%, Fe_2O_3 content less than 10%, with LOI shall be less than 5%, and reactive silica content shall be in the range of 40–50%. FA fineness shall be in the range of 80–90% of particles smaller than 45 μm. Researchers have claimed that FA particles below 10 μm show more reactivity and higher strength for 7 and 28 days [21,72]. The FA up to 428 kg/m^3 show better performances in GPC with CS value achieved as 49 MPa for day 7. MK is a waste produced through alumina extraction from bauxite ores through the Bayer process. RM enriches in sources as, Al_2O_3, SiO_2, and Fe_2O_3, with the mineral of zeolites, quartz, mainly consisting of calcium and sodium along with clays, hematite, etc. [73] These ingredients are suitable for polymerization production and RM efficient in refineries with low Al_2O_3 results in alkali-activation [74]. RM used along with rice husk ash as a binder has CS up to 20.5 MPa. The constituent of the RHA is SI which is amorphous along with partially crystalline phases. RHA has high-surface-area particles. RHA has small trace elements, i.e., K and Ca. RHA, with amorphous nature, is reactive and acts as a pozzolanic. Use of RHA the GPC have CS up to 56 MPa depending on the content of FA and RHA, fineness of RHA, and molar concentration. RHA-based GPC has better performance than other binders such as glass powder [59,72–74]. Utilization of silica fume ranging from 20% to 25% led to better performances of GPC on strength properties. Silica fume is finely discrete amorphous SiO_2, the surface of which is enclosed by silanol with help in increase in the rate of reaction in the matrix. GGBS is a by-product of iron production at blast furnaces, comprising Si majorly, Al, and Ca in chemical composition [16,19,20,75]. The introduction of GGBS as a binder in GPC develops the reactivity of low-calcium content with FA [72,76]. Calcium-rich aluminosilicates speedy setting and leads the high early strength. Clays and other natural minerals are also better sources of aluminosilicates for the preparation of GPC. Kaolin in its dehydroxylated form, MK, rich in aluminosilicates sources which is more suitable for polymer preparation[56].

A few of the activator agents used to produce a GPC are NaOH, Na_2SiO_3, K_2SiO_3, KOH, Na_2SO_4, $CaSO_4$. Utilization of Na_2SO_4, NaOH, $CaSO_4$ as activator agents can produce CS up to 33 MPa under oven-cured conditions subjected to 64 °for 45 hrs [73,78]. When the cubes are subjected to oven-cured at 25–28 °, it results in the development of CS up to 26 MPa. RHA on FA-GGBS based GPC as binder with Na_2SiO_3 and NaOH as activators result in 56 MPa as CS. Using a KOH activator also results in comparable CS [63,79,80]. The activation agent plays a remarkable role in the rate of polymerization. For instance, the solubility of Al^{3+} and Si^{4+} ions are more excellent in NaOH, but in the case of KOH, it's lower despite the same molar [74,80].

7. Activator agent effect on environment

The dumping of agricultural and industrial waste products has become a major environmental concern. The waste is generated during the polishing of flat glass plates, which are commonly used in civil construction projects. A medium-sized company's yearly production of glass polishing trash is around 84 tons, causing environmental degradation on a massive scale when multiplied by a significant number of firms throughout the world. Glass polishing waste is typically disposed of in landfills. In ecological ceramic roof tiles glass polishing waste utilized as a partial replacement for raw material such as fly ash via the geopolymerization process [90]. Previously, some researchers employed this sort of waste for absorption in cementitious materials, such as mortars for building projects, with the goal of evaluating the impact of the waste. With the goal of using rheological testing to assess the impact of glass waste integration on the rheological characteristics of adhesive mortars. However, there enough research on the durability of geopolymers including glass polishing waste need to be done.

Due to the lower cost and availability of sodium-based compounds compared to potassium-based compounds, sodium hydroxide and silicate are utilized more frequently. However, because of the production process, the usage of these commercial goods increases the energy incorporated and CO_2 emissions associated with alkali-activated binders. The chlorine-alkaline method, which involves electrolysis of seawater, is used to make sodium hydroxide. According to an emission measurement conducted in an Australian firm, the manufacturing of 1 kg of commercial NaOH emits 1.915 kg of CO_2. The calcination of silica sand and sodium carbonate at temperatures between 1400 and 1500 °C is then used to make sodium silicate [91]. The overall CO_2 emissions are projected to be in the billions of tones. Although alkali-activated binders have a smaller CO_2 footprint than Portland cement and epoxy resin-based binders, the usage of industrial silicates, such as sodium silicate, adds to an increase in CO_2 and energy emissions connected with their manufacturing. It happens because of the way these substances are made. In addition, the great majority of these materials are hazardous due to high pH and toxicity, and they are costly. As a result of this circumstance, novel activators made from waste (industrial or agricultural) or low-cost materials rich in silica and/or alkaline cations have been developed (sodium and potassium). One of the most important characteristics of these materials is that they are soluble, allowing the release of the ions required for the development of alkaline activation. Furthermore, it is required, to stimulate the dissolution of aluminate and silicate ions and hydrolyze the surface of the raw material particles, the activating solution must have a pH high enough. The total CO_2 emission per kg of sodium silicate generated conventionally is estimated to be roughly 1.514 kg.

8. Influences of the ratio of sodium silicate to sodium hydroxide (SS/SH)

The SS/SH was considered as 2 and 2.5 for GPC. The maximum CS value was observed for 2 ratios up to 30 MPa strength was achieved for day 3. Researchers had investigated using FA as binding materials, and they varied the SS/SH ratio ranging 1.75–3. They witnessed that maximum CS was achieved at 2.5 ratios at ambient temperature [81,86]. They were only a marginal increase in CS value between 2.5 and 3. The effect of temperature as curing condition in SS/SH ratio was investigated for 60, 75, and 90 °for 24 hrs to 48 hrs as exposure duration. They found that maximum CS value was achieved for an SS/SH ratio of 2.5 with 75 degrees for 24 hrs duration [82,87]. GPC exposed to ambient temperature and oven-cured condition the CS value increases with increase in SS/SH ratio up to an optimum point beyond that CS start to reduce. For 14 M with the oven-cured specimen, the maximum CS value for 56 days is

35.7 N/mm^2. Similarly, for 16 M with ambient cured specimen, the maximum CS value for 56 days is 25.8 N/mm^2. The maximum CS value was found for specimen exposure to oven-cured than the ambient cured temperature [44,83]. STS test was carried out for different SS/SH ratios such as oven cured and ambient cured along with varying the SS/SH ratio ranging 0.5–3.0. Maximum STS was observed for 2.5 with 4.2 MPa for oven-cured compared with 2.5 with 5.2 MPa for the ambient cured specimen [11,84,88]. SS/SH ratio ranged from 0.5–3.0. STS was also increased to ratios SS/SH of 2.5 for ambient and over the cured specimen. The SS/SH ratio ranging from 0.5 to 3 with the interval of 0.5 was investigated on the curing condition of GPC, such as ambient and oven condition. For SS/SH ratio 2.5 with 5.6 MPa as maximum FS was observed for oven-cured condition. For SS/SH ratio 2.5 with 4.0 MPa as maximum FS was observed for ambient-cured conditions. As the SS/SH increases up to 2.5, the FS increases for both curing conditions [64,85]. An increase in SS/SH reduction of STS for 28 days was observed [86,89]. The decrease in 28-day STS is 10.1% for 0.4 ratio and 20.5% for 0.50 SS/SH ratios compared with 0.30. Water absorption(WB) was higher for 0.50 compared with 0.40 and 0.30 ratio [87,90]. SS/SH ratio with 0.4 had 9.3% and 0.50% had 11.3% of WB higher compared with 0.3 ratio. As the SS/SH ratio reduces, the structural performance of GPC decreases due to sodium silicate reduction in the geopolymer reaction [64,88].

9. Influences of the ratio of alkaline to binder (A/B)

The most common activator used for the preparation of GPC is a combination of $NaSi_2O_3$ and NaOH [82,89]. Activators have a significant impact on the polymerization process. Polymerization takes place at a high rate when the alkaline activator dissolves the Si and Al from binding material to form the matrix. Activator prepared using the NaOH and Na_2SiO_3 improved the reactivity in FA [90,91]. The performance of the GPC was better while using a superplasticizer on the strength property. A/B ratio for 0.4 had maximum CS compared with 0.30. The author investigated GPC using FA as binding materials, various the A/B ratio ranging from 0.25 to 0.40. They concluded that maximum CS was achieved at a 0.35 ratio at ambient temperature [91,92]. They were only a marginal increase in CS value between 0.35 and 0.40. The effect of temperature as curing condition in A/B ratio was investigated for 60, 75, and 90 °for 24 hrs to 48 hrs as exposure duration [99]. They found that maximum CS value was achieved for an A/B ratio of 0.35 with 75 °for 24 hrs duration. A/B ratio has a prominent result on GPC at the initial slump [45]. The intensification in the A/B ratio increases the slump. 0.4 And 0.5 SS/SH ratios were investigated on the slump. The effect of the A/B ratio on 28-day STS property was investigated [32]. The increase in the A/B ratio yields high STS. As STS value increases with increase in A/B ratio up to 0.4 beyond which a reduction of STS values. The A/B ratio for 0.35, 0.40, and 0.50 had STS value of 49.5%, 60.3%, and 52.2% increment when compared with 0.30 A/B ratio. Lower A/B ratio of significances in the lower structure performance of the GPC [100,101]. This led to the detail that collective modulus causes a weaker activator and slower polymerization rate, resulting in a decrement in the polymerization reaction. The lesser the formation of gel in the matrix eventually reduces the mechanical performance of GPC [89].

10. Curing conditions

There have been several attempts to study the effects of various curing processes on the characteristics of geopolymer pastes. Complete Geopolymerization reactions were observed to cure at 40–85 °C. At 65 °C and 85 °C, activator agent (0.25 and 0.30 liquid/solid ratio) was cured [21,95,102]. They found that molar with (8–12 M) treated at 85 °C for 24 hrs had significantly better compressive strength than those cured at 65 °C. When the curing time was increased after 24 hrs, the increase in strength was substantially lower [28,29,32]. Curing metakaolin-based geopolymers at room temperature proved impossible; however increasing the temperature (40 °C, 60 °C, 80 °C, 100 °C) favors strength gain after 1–3 days. Curing at a higher temperature for a longer length of time, on the other hand, resulted in sample failure at a later age due to thermolysis of the Si–O–Al–O bond [35].

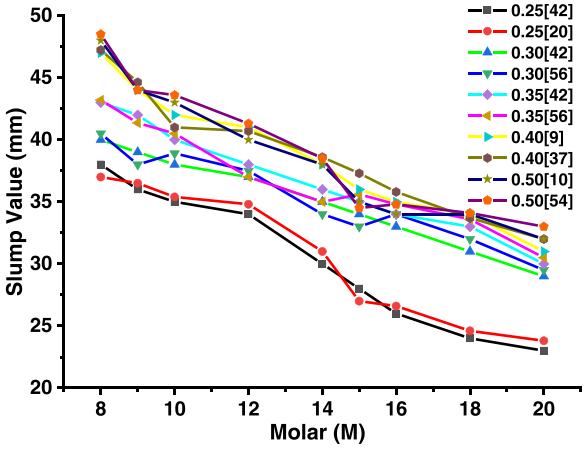

Fig. 3. Effect of a molar on slump by variation of A/B ratio.

11. Influence of molarity on the slump

The variation of molar and A/B ratio on the slump test results data were collected from past research papers. Data was compiled and represented as shown in Fig. 3**.** The different molar such as 8, 10, 12, 14, 16, 18 and 20 M with 0.25, 0.30, 0.35, 0.40, 0.50 as A/B ratio were considered for the present study. As the molar concentration increases, the slump starts to reduce. The maximum slump was observed at 8 M, and the minimum slump at 20 M. The slump value can be increased by adding admixture to the mix along with binder type also plays a major role in the higher slump. For the A/B ratio of 0.50 and 0.40, there is a marginal increment and decrement of a slump. Molar concentration increases along with increases in the A/B ratio, slump results decrease.

GPC prepared with FA as a binder has more density than MK. This happens mainly due to FA spherical shape particle and porous structure. FA has high fineness resulting in enhanced workability [86]. The effect of different molar concentrations was investigated on FA-based GPC. They used 12, 16, and 18 M for the study. They concluded that as the molar concentration was increased the slump value was decreased. For12 M shows the maximum slump; polymer matrix has a stiff consistency in the new state [103]. The use of admixture observed improvement in the workability. The naphthalene sulphonate-based superplasticizer enhances the slump. The range of plasticizer used was from 2% to 4.5%, as the dosage of plasticizer was increased the slump value was also increased [93]. For 4.5 dosage, the maximum slump was observed with 240 mm. Researchers also observed that admixture at 2% dosage has maximum CS value. Beyond 2% dosage, the CS starts to decline.

Aggregate content in the polymer paste affects the fresh property of GPC, such as workability. When silicate reacts with free Na^+ ions in the gel results in the formation of soluble phases of NASH gel due to excess sodium silicate, cracks develop in the matrix [5,8,9]. The particle shape of the binder has a more significant impact on the structure performances of GPC. MK was more irregular than spherical and had an edged shape leading to a lower slump. A higher concentration of molarity significance intensifies the viscosity of NaOH [92]. FA mixed with NaOH agent causing to cohesive and sticky GPC. 16, 14, and 12 M shows lower slump value related with 10 and 8 M, due to the lower ratio of Na_2SiO_3/NaOH. As the molarity of an activator is increased, the slump performances lower [102, 104]. Higher content of CaO in MK led to the rapid development of the setting timing due to the formation of the C-A-S-H structure, which reduces the slump value.

MK indicates heterogeneous microstructure and particles from agglomeration and makes dense with diverse particles [60]. MK and GGBS binders are rich in Na ions with increment Na/Al molar ratio during fusion progression. GGBS reacts with silica, leading to a new crystalline phase [105]. Alkali fusion of GGBS, some mineral phases transformed into amorphous, and new crystalline phases formed in the matrix. Unreacted ions of Na+ defined their paths in this way, either agglomerated or migrated at the boundary of remained. MK particles become less dense after the fusion process [106].

12. Influence of molarity on compressive strength (CS)

The variation of molar and A/B ratio on the compressive strength test data were collected from past research papers, data was compiled to study the pattern, and the same is represented for 7, 14, and 28 days as shown in Figs. 4, 5**,** and 6**.** Different molar such as 8, 10, 12, 14, 16, 18 and 20 M with A/B ratio as 0.25, 0.30, 0.35, 0.40, 0.50 for 7, 14 and 28 days of CS considered for the present study. As the molar concentration increases, the CS value increases up to a certain limit. The maximum CS was observed at 16–18 M and the minimum CS at 5 M for 7, 14, and 28 days. Higher CS can be achieved by appropriately utilizing factors such as A/B, SS/SH ratio, and binder type. For the A/B ratio of 0.50 and 0.40, there is a marginal increment and decrement of a CS. A/B ratio of 0.40 maximum CS is achieved for 7 days, but 14- and 28-days A/B ratio of 0.35 had maximum CS. Molar concentration increases along with increases in the A/B ratio up to 0.40, CS increases.

The author had investigated GPC using 8 M, 10 M, 12 M, and 18 M. CS, and the workability of GPC was measured. For 14 M, the maximum CS value was observed with 46 MPa for day 7. The molar concentration increase the CS value also increases. An increase In the GGBS content led to an increase in calcium oxide in the matrix [87]. Other oxides such as silica and alumina enhance the CS

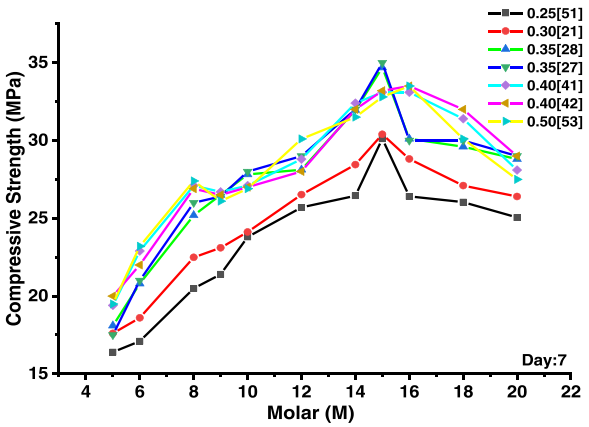

Fig. 4. Effect of a molar on CS by variation of A/B ratio for day 7.

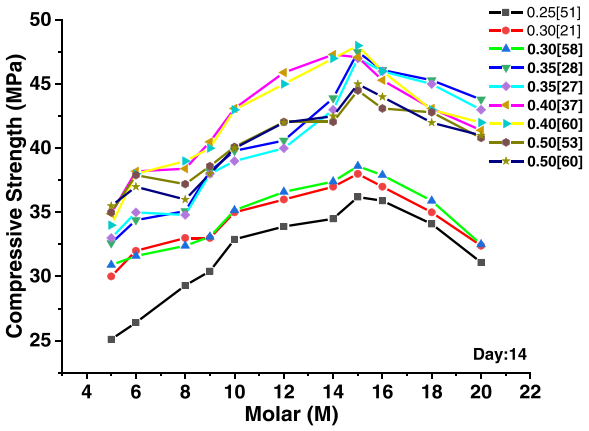

Fig. 5. Effect of a molar on CS by variation of A/B ratio for day 14.

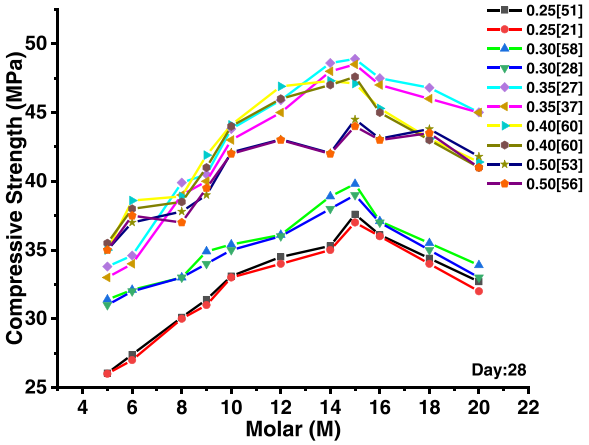

Fig. 6. Effect of a molar on CS by variation of A/B ratio for day 28.

property of GPC. The high content of Ca and Al in the matrix results in the formation of (C-S-H) gel along with great extents of tetra-coordinated in the interlayer spaces [27]. Hence, higher CS is achieved; matrix composition and molar significantly impact CS. The binder combinations, such as glass powder and GGBS, led to the development of 25 MPa strength for 28 days at ambient curing. For 12 M NaOH encompasses discrete hair cracks in the microstructure of matrix then compared with 4 and 8 M. They concluded that compact microstructure was observed for 4 M mix for higher GGBS and lower GP content improves the rate of hydration in the matrix

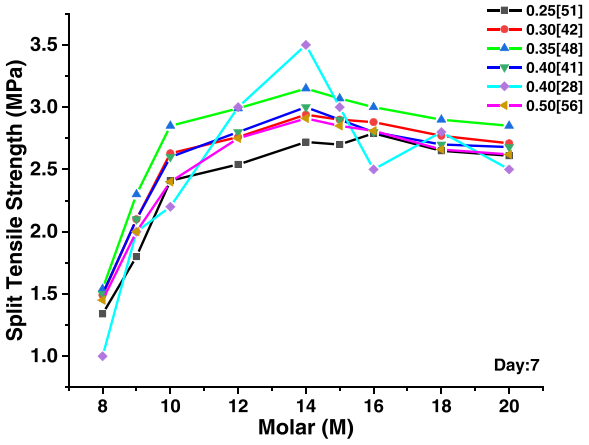

Fig. 7. Effect of a molar on STS by variation of A/B ratio for day 7.

[68]. Al and Ca content reduces in the matrix due to the reduction in the proportion of GGBS; subsequently, strength reduces. Ca and Al presence in the matrix led to the development of N-A-S-H. The higher proportion replacement of FA with GGBS in the matrix reveals better results [43]. The additional increment in a molar from 8 M to 12 M causes a decline in the rate of hydration. A higher amount of GGBS usage beyond 60% led to diminished CS. Less GGBS and the increase in molar reveal the weaker ITZ followed by hair-line crack observed at the micro level [107]. CS value of GPC depends on these factors, such as molarity of activator and curing condition. GPC exposed to oven-cured condition the CS value increases with increase in molarity up to an optimum point beyond that CS start to reduce [108]. For 14 M with the oven-cured specimen, the maximum CS value for 56 days is 34.2 N/mm^2. For 16 M with ambient cured specimen, the maximum CS value for 56 days is 25 N/mm^2. The maximum CS value was found for 16 M as 25.0 N/mm^2 for ambient-curing compared. The maximum CS value was found for 16 M with 31.0 N/mm^2 for oven-curing compared at 56 days.

FA and GGBS, when mixed with sodium hydroxide, show better performance. As the molarity is increased from 8 to 16 M, the CS value also increases. The effect of molarity on the CS property of GPC was investigated for 7 and 28 days. The molarity used for GPC was 12–18 M with an interval of 2 M [109]. The cube was cured at 50 ° before CS tests were carried out. The growth in 28-day CS was 45.7% for 16 M, and CS was 9.10% for 18 M for 28 days; 16 M shows better performances than 18 M [110].

13. Influence of molarity on split tensile strength (STS)

The variation of molar and A/B ratio on the split tensile strength test data were collected from past research papers, data was compiled to study the pattern, and the same is represented for 7 days, as shown in Fig. 7. It represents the different molar such as 8, 10, 12, 14, 16, 18, and 20 M with A/B ratio as 0.25, 0.30, 0.35, 0.40, 0.50 for 7 days of STS considered for the present study. As the molar concentration increases, the STS value increases up to a certain limit. The maximum STS was observed at 16–18 M and the minimum at 8 M for 7 days. Higher value STS can be achieved by appropriately utilizing these factors such as particle shape and size, mixing method of GPC, and curing condition. For the A/B ratio of 0.30 and 0.40, there is a marginal increment and decrement of an STS. A/B ratio of 0.35 maximum STS is achieved. Molar concentration increases along with increases in the A/B ratio up to 0.35, and STS increases for 7 days.

Average growth of around 70% in the SPT was witnessed for all the composite mixes related to the control mix, signifying the formation of -Ca–Si–Al gel in the matrix. FA as binder and activator with 12 M led to maximum STS as 1.70 MPa at 28 days compared with 8 M and 4 M [88]. The STS was increased for glass powder content up to 10% with increasing molar from 4 to 12 M. STS test was carried out for different curing conditions such as oven cured and ambient cured along with varying the molar from 8 M to 16 M. Maximum STS was observed for 14 M with 5.2 MPa for oven-cured compared with 16 M with 3.6 MPa for ambient cured specimen [26]. As the molar concentration was increased from 8 to 16 M, the STS was also increased for ambient and over the cured specimen. The effect of molarity on GPC with STS properties was investigated for 28- days with 48 hrs of curing at 50 °. For 16 M, STS was 44.7% higher, and for 18 M, STS was 2% higher when compared with 12 M. Molar concentrations, alkaline to binder (A/B) ratio, and Na_2SiO_3/NaOH ratio has a vital role in the enhancement of strength during polymerization [105,106]. The increment of higher molarity enhances the pH in the matrix, which favors the growth of amorphous phase development. A lower molarity ratio results in lesser strength development in the matrix due to the lesser Si and Al ion dissolution. With 16 M and 0.50 A/B ratio, there is an intensification in Si and Al ions leaching from GGBS, subsequent formation of N-A-S-H gel in the 3-D framework [10,107]. Dense and robust polymer paste is achieved by increasing FA. The impact of changing molar in the matrix signifies that an increase in dissolution silica and alumina results in higher STS and FS. Attribution to the reaction kinetics of GGPC. As the ratio of molar and A/B contribute more effectively to polymerization, beyond certain limits, further increases lead to the decrement of performances of GPC [11,18,32,75,108].

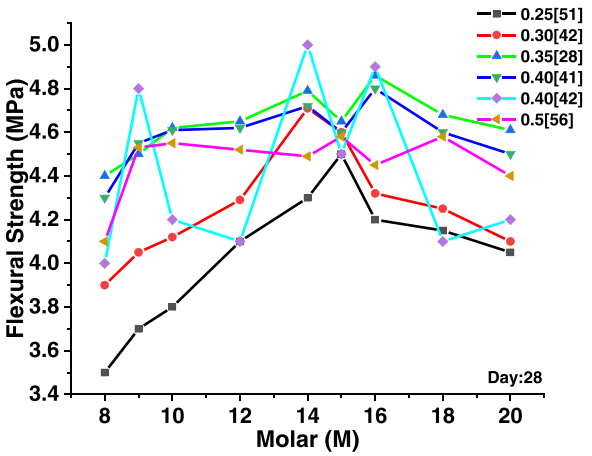

Fig. 8. Effect of a molar on FS by variation of A/B ratio for day 28.

14. Influence of molarity on flexural strength (FS)

The variation of molar and A/B ratio on the flexural strength test data were collected from past research papers, data was compiled to study the pattern, and the same is represented for 28 days, as shown in Fig. 8**,** represents different molar such as 8, 10, 12, 14, 16, 18, and 20 M with A/B ratio as 0.25, 0.30, 0.35, 0.40, 0.50 for 28 days of FS considered for the present study. As the molar concentration increases, the FS value increases up to a specific limit. The maximum FS was observed at 16–18 M and at 8 M for 28 days. Higher value FS can be achieved by appropriately utilizing these controlling factors such as types and size of fine and coarse aggregate, mixing method of GPC, and curing condition. For an A/B ratio of 0.35 maximum, FS is achieved. Molar concentration increases along with increases in the A/B ratio up to 0.35. FS increases for 28 days.

12 M, FS for 7 and 28 days, the specimens were observed to be broken during the time of demolding. This happened mainly owing to the minor reactivity of FA at ambient temperature, resulting in lesser strength improvement during the phase of demolding. Glass powder with 5% as a molar increment from 4 to 12 M, FS values reduce at 28 days. FS for 28-day has a lesser value than day 7 [106, 108]. Due to the high shrinkage in the matrix, this matrix includes a higher quantity of unreacted FA particles. Lower water requirement and the gel environment of the binder, a better quality of GPC than conventional concrete [113]. GPC has a lower rate of hydration while setting. Another significant factor is the development of micro-cracks in ITZ. These micro-cracks influence FS as associated with CS, decreasing the FS with age [106,109]. FS specimens were cured at ambient temperature does not withstand their weight after demolding.

Failure of beam specimens found to be brittle mode. FS value was found to be maximum for oven-cured compared with ambient cured specimens [79,109]. The different molar concentration of 8–16 M with the interval of 2 M was investigated on the curing condition of GPC, such as ambient and oven condition. For 14 M with 5.4 MPa as maximum FS was observed for the oven-cured condition. For 16 M with 3.9 MPa as maximum FS was observed for ambient-cured conditions. As the molar concentration increases the FS also increases for both curing conditions. More viscous activator agent results in a decrease in the unreacted particle of GGBS in the matrix. Due to this, there is strong bond development between silica and alumina ions. The Na_2SiO_3/NaOH ratio is decreased, making sodium silicate is less viscous than sodium hydroxide decreased resulting in the decrement of FS [32,114].

15. Influence of molarity on water absorption (AB) and bulk density (BD)

Water absorption (WB) and bulk density (BD) test for different molar and A/B ratios data were collected from past research papers, and data was compiled to study the pattern, as shown in Figs. 9 and 10**,** represents different molar such as 8, 10, 12, 14, 16, 18 and 20 M with A/B ratio as 0.25, 0.30, 0.35, 0.40, 0.50 for WB and BD considered for the present study. The WB and BD value increases as the molar concentration increase up to a specific limit. The maximum WB and BD were observed at 18 M, and the minimum WB and BD at 8 M. Higher WB and BD can be achieved by appropriately deploying these factors such as specific gravity of binder and particle size distribution curve for binder. For the A/B ratio of 0.50 and 0.40, there is a marginal increment and decrement of a WB. A/B ratio of 0.40 maximum WA is achieved. For an A/B ratio of 0.50, the maximum BD was achieved.

Molarity of mixes increased in the density of the specimens also increase up to 14 M, but beyond the 14 M reductions, the density specimens. For ambient curing, 16 M of GPC had a maximum density of 2482 kg/m^3 for 28 days, but for oven-cured density was found to be 2474 kg/m^3. The effect of molarity on WA on 28-day results shows that WA values reduce with the increment in molarity ranging 12–18 M. For 16 M and 18 M, the WA was 5.4% and 1.4% higher compared with 12 M. For 16 M shows maximum WA compared with other molars [31,52,110]. The enhancement in GGPC strength is a consequence of the increased NaOH to Na2SiO3 ratio, due to which sodium silicate enhances the polymerization, resulting in a rapid chemical reaction with higher structural properties [115]. Soluble silicates added to high alkali concentration enhance the ITZ bonding between binder and aggregates. Intensification in the liquid/solid

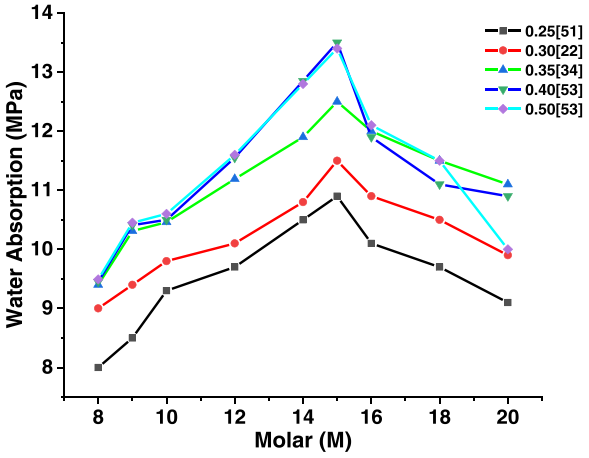

Fig. 9. Effect of a molar on AB by variation of A/B ratio.

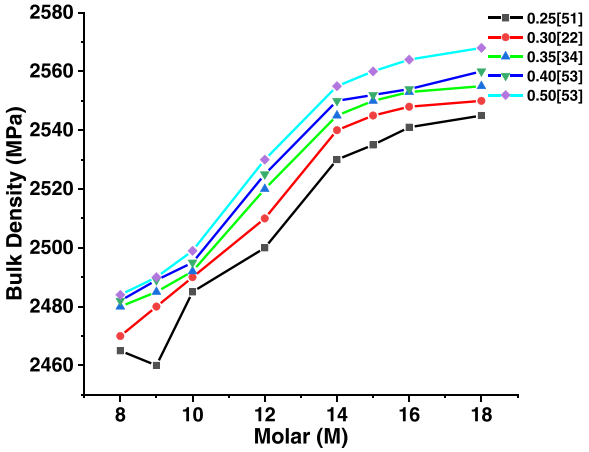

Fig. 10. Effect of a molar on BD by variation of A/B ratio.

ratio leads to a decrement in the molar and alkalinity of the activator, along with declines in the influence on the MK-GGBS matrix [77, 110]. However, increasing the ratio of liquid/solid reduces a larger size of pores in the macrostructure; thus, dense GPC is achieved. Abundant silicon in the GGBS and MK also consists of a certain extent of CaO, which is fewer in MK whereas more than GGBS [116]. Reactive alumina led to react with the alkaline agent to produce geopolymer gel. The access of vibration carried out during GPC resulted in bleeding of the geopolymer paste and brought gel upward. The effect of aggregate inhibits gel from dissipating, causing high gel content into the aggregate bottom [76,111]. The presence of gel below aggregate leads to lower activator molarity, weaker alkalinity, and slower polymerization, developing a binder with a porous structure. An increase in the A/B ratio reduces the absorption property of GPC [71,112]. For 0.35, 0.40 and 0.50 A/B ratio the AB was 8.6%, 12.2% and 11.2% for GPC matrix. The enhancement in GPC properties is a cause of the increasing A/B ratio. The increase in the A/B ratio increases the content of Si because the activator contained sodium silicate, which led to an enhancement in the SiO_2/Al_2O_3 in matrix and makes Si-O-Si bonds stronger [117].

16. Effect of fibers in geopolymers

Davidovits was the first to investigate the use of fibers to strengthen geopolymer composites, with the goal of producing moulds and patterns for the plastics processing sector. In the automotive and aerospace sectors, as well as in naval design, fiber-reinforced geopolymer matrices play a significant role as a cutting-edge technical solution [118]. Synthetic fibers like steel, glass, and carbon fibers are the most prevalent geopolymer reinforcing fibers. Additionally, several studies have been conducted to examine the utilization of polymeric fibers such as polypropylene and polyvinyl alcohol fibers [119].

17. Polypropylene fiber

A recent study looked at several geopolymer mortars that were reinforced with polypropylene fiber (PP) and dosed with different silica modules of 0.8, 0.9, and 1.0 and molar ratios of 12, 14, and 16 M, with PP fibers added at varying levels. Past study shows that an ideal combination with a molar ratio of 16 M and 0.5% PP fiber volume produced good results with high viscosity, significant adhesion, and mechanical flexural strength. There was also a reduction in voids when temperature changed, and calcium silicate hydrates (CSH) gels assisted in the geopolymerization process [118].

18. Natural fiber

The use of natural fibers to reinforce geopolymer composites is relatively new, and it is primarily motivated by a rising concern towards environmental preservation and a desire to create more sustainable construction materials. Natural fibers are useful in this circumstance since they are renewable, biodegradable, and non-toxic, as well as having a low density and enough mechanical strength. Furthermore, the economics of replacing synthetic fibers with natural fibers are intriguing, considering that the manufacture of artificial fibers is an energy-intensive operation compared to the planting and harvesting of natural fibers. When natural fibers are used as reinforcement in geopolymer matrices, the hydrophilic and hydrophobic behaviour of the fibers might impact fiber–matrix adhesion, just as it does with synthetic fibers. Natural fibers are hydrophilic by nature due to the presence of hydroxyls and other polar groups; yet, cellulosic fibers have a high moisture absorption rate and low dimensional stability because they swell when exposed to water. This phenomenon causes not only a weakening of fiber–matrix adhesion, but also the creation of fractures when the composite dries, as well as a decrease in mechanical performance [118,119,121].

19. Steel fibers

Geopolymer pastes and steel microfibers, as well as polypropylene fibers, form an interfacial connection. It was able to detect a smoother and more regular surface in the polypropylene fiber, which does not contribute to a strong adhesion between the fiber and the matrix [82]. Steel micro-fiber, on the other hand, had a considerably rougher and coarser surface and demonstrated higher adhesion to the matrix. The results of the flexural strength tests show that the surface of the fibers and the fiber–matrix interface are related: slurries reinforced with steel microfibers had higher strengths than the reference for most fiber insertion contents tested, whereas samples containing polypropylene fibers showed a decrease in strength for all contents except 4%. Because the geopolymer paste is a water-based substance, the tendency of steel and polypropylene fibers to absorb or resist (hydrophobia) water can be a determinant for a strong connection between the reinforcing fiber and the geopolymer [89]. The surface of the polypropylene fiber is hydrophobic, whereas the surface of the steel microfiber is hydrophilic, according to the angle of contact with water on the surface of each fiber. With low mechanical performance of pulps reinforced with polypropylene fibers, it is reasonable to conclude that the regular shape of the fiber surface, together with its hydrophobic activity, resulted in a weak fiber–matrix contact [123].

20. Influences of ferrosialate in geopolymerisation process

Tunnels, high-rise buildings, nuclear power plants, and other constructions require a high level of thermal resistance. The resilience of OPC structures to high temperatures is quite low. Between 100 and 150 °C, its microstructure begins to deteriorate [120]. Previous research has shown that FA based GPC are more resistant to high temperatures than OPC concrete. Polysialate and ferrosialate can occur when polysialate and ferrosialate are cured at low temperatures (ambient) while preparing GPC [23]. However, residual iron hydrate or oxyhydrate, as well as Oligomers, may persist in the matrix, causing inadequate densification. With the use of steam curing at a high relative humidity (80 °C, RH 80%), the systematic removal of iron oxyhydrate and hydrate with the increase of ferrosialate concentration is obtained [103]. The concentration of nano iron silicate was dramatically enhanced when there was a high concentration of reactive silica Curing at temperatures between 50 and 100 degrees Celsius improves the transition of hydrates and oxyhydrates to ferrisilicates, as well as the creation of ferrosialates and polysialates. Ferrosialate geopolymer samples had a maximum CS of 53.34% greater than sialate GPC The oxide ratios of $SiO_2/Al_2O_3 = 4.0–4.3$, $Na_2O/SiO_2 = 0.15–0.17$, and $Fe_2O_3/Al_2O_3 = 0.27–0.37$ have been discovered to constitute limitations for maximum strength growth [89,117].

21. Effect of molarity of geopolymers mortar (GPM) interferes with the durability properties

21.1. Saturated solution immersion method

By immersing the mortar in a saturated solution, the durability of the mortar may be determined. There is considerable mass loss of geopolymer matrix after immersion in a saturated solution of NaCl, according to the results of mass loss and strength of GPM following durability testing with immersion in a saturated solution of NaCl [121]. The mass loss in reference mortars is greater, especially at a SiO_2/Al_2O_3 ratio of 3.0. whereas for a 2.5 ratio of SiO_2/Al_2O_3 reference mortar cured under ambient conditions, the smallest mass loss is found. For the same curing conditions and SiO_2/Al_2O_3 ratio, the mass loss of specimens treated under condition B is smaller than that of specimens processed under condition A [91]. After immersion, the reference mortar has the maximum mass loss of 40.20%, whereas the mortars with processing conditions "A" and "B" at the same time had the lowest mass loss. Furthermore, when compared to ambient curing, GPM conditioned at heat curing lose more mass. Curing at a high temperature produces some deterioration of the specimens, resulting in a mass loss. Thermal curing results in a 4–6% greater loss of mass of specimens than ambient curing once the immersion cycles are completed. Furthermore, for ambient curing, GPM with a SiO_2/Al_2O_3 ratio of 2.5 has a higher mass loss than mortar with a SiO_2/Al_2O_3 ratio of 3.0. It's also worth noting that mortars made with a SiO_2/Al_2O_3 ratio of 2.5 and processed under condition "A" lost more mass. In comparison, a mortar made with a SiO_2/Al_2O_3 ratio of 3.0 and processed under condition "A" lost more mass.

21.2. Thermal shock

After the durability test, when specimens were subjected to thermal shock, mass loss and strength of GPM specimens were measured. The geopolymer mortar specimens were treated to a total of 120 days of thermal stress, which included 24 h in a 200 °C oven followed by 24 h in a 0 °C refrigerator [56]. The results in Fig. 6 show that thermal shock has a lower impact on mass loss in GPM. The reference specimens cured under ambient and heat settings for 2.5 ratio of SiO_2/Al_2O_3 lost the least amount of mass, followed by the specimens prepared under processing condition B for the same curing circumstances and ratio of SiO_2/Al_2O_3. It implies that the mortars are more robust in terms of mass loss resistance during thermal shock situations [59–61]. The GPM with a 2.5 SiO_2/Al_2O_3 ratio and ambient curing loses the most mass when manufactured using processing condition "A." Furthermore, mortars with a SiO_2/Al_2O_3 ratio of 3.0 manufactured under processing conditions "A" and "B" yielded similar results, but were superior to reference mortars under the same conditions [50,89].

22. Microstructure analysis

22.1. Scanning electron microscope (SEM)

The use of Si and nano-Si as fillers filled porosity gaps and enhanced packing particles between the binder phase, FA-fly ash, and GGBFS-ground granulated blast furnace slag, according to the researchers. As a result, this cohesiveness appears to prevent the weak link between them [35,46,112]. The ITZ generated by the absence of binder phase into the matrix in both GPC resulted in reactive and unreacted particles in both geopolymer concrete. The former in GGPCSF1.5 comprises Na, O, and Si attributable to polysialate N-A-S-H gel, whereas the latter contains Na, O, and Si attributable to polysialate N-A-S-H gel [40,122]. On a microscope of the GGPCSF1.5 sample, however, was noticed white needle crystals related to NaOH or Na_2SiO_3. The creation of sodium carbonate from non-reacted

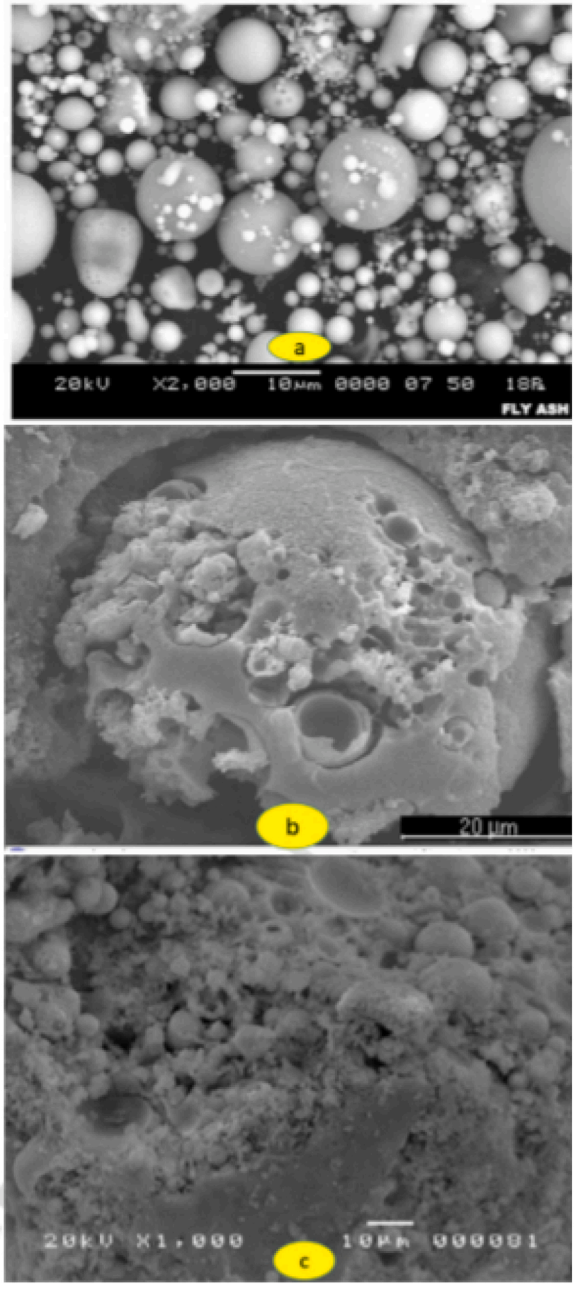

Fig. 11. SEM images (a) FA, (b)FA with 8 M,NaOH for 20hrs at 86 degree. (c) FA activated with Na_2SIO_3. (reproduced with permission [58]).

Na in geopolymer reactions with atmospheric CO_2 or the precipitation of Na_2SiO_3 from an excess of reactive silicate with sodium ions might explain the needle forms. As a result, the microstructure evolution in both geopolymer specimens corresponds to the strength development trend [59,71,114]. Fig. 11 shows the fractures of GGPCSF1.5 and GGPCNS1.5 samples, which show their interior texture in detail (a-b). Both micrographs seem heterogeneous, compact, and dense, indicating a high degree of cohesiveness between the binder phase and coarse particles, which explains the good mechanical performance. On both specimens, there were no fissures or cracks, which indicates that there is a significant quantity of binder phase that allows for good adhesion or bonding between various particles within the matrix framework [87,123,124]. Thus, using Si and nano-Si as silica sources resulted in a greater degree of geopolymerization and polycondensation, resulting in good densification of the entire system and high strength development. According to the researchers, this pattern has been seen by many authors. The use of Si and nano-Si as fillers filled porosity gaps and enhanced packing particles between the binder phase, FA and GGBS [25,63,73,116]. As a result, this cohesiveness appears to prevent the weak link between them. The ITZ generated by the absence of binder phase into the matrix in both GPC resulted in reactive and unreacted particles in both geopolymer concretes. The primary components in GGPCNS1.5 sample (Fig. 13b) corresponding to -N-C-S-H, -N-A-S-H, -C-S-H, and $Mg(OH)_2$ binders type, while the latter in GGPCSF1.5 comprises Na, O, and Si attributed to polysialate -N-A-S-H gel are Al, Si, Ca, Mg, O, and Na. On the microscopy of the GGPCSF1.5 sample, however, was noticed white needle crystals associated with NaOH or Na_2SiO_3 (Fig. 13a). This needle shape might be caused by unreacted Na in geopolymer reactions with ambient CO_2, leading to sodium carbonate production or sodium silicate precipitation [57,99,116]. Due to an excess of reactive silicate in the presence of sodium ions as a result, the microstructure evolution in both geopolymer specimens corresponds to the strength development trend [86,116].

22.2. XRD analysis

The GPC sample mixed with OPC as a FA substitute underwent XRD examination. The phases were recognized using High score software, as shown in Fig. 12 a and b is for unexposed sample and sample exposed to the sulfuric acid solution for 365 days. Sharp peaks and a minor quantity of C-A-S-H were detected in the unexposed specimens with 0% OGPC, indicating crystalline phases of quartz, mullite, and nepheline. Quartz, nepheline and mullite, were discovered when the identical samples were subjected to sulphuric acid for 365 days, albeit with lower intensities [44,87,97,116]. The geopolymerization process involves polymerization events that produce alumina-silicate solid linkages; they were exposed to sulphuric acid for a more extended time, and the aluminosilicate polymers depolymerized, causing the material to deteriorate.

Furthermore, past research has shown that geopolymer concrete has more excellent acid resistance than traditional concrete after completing XRD characteristics. The introduction of OGPC to the geopolymer system resulted in a decrease in quartz and mullite in unexposed samples but an increase in nepheline and a new peak portlandite. In addition to the broad humps that proved its coexistence with the polymeric binders, the new peak can be attributed to the calcium-based hydrated product [13,61,102,116]. The 10% OGPC geopolymer concrete specimen exhibited the existence of quartz, mullite, and nepheline with decreasing intensity and the addition of

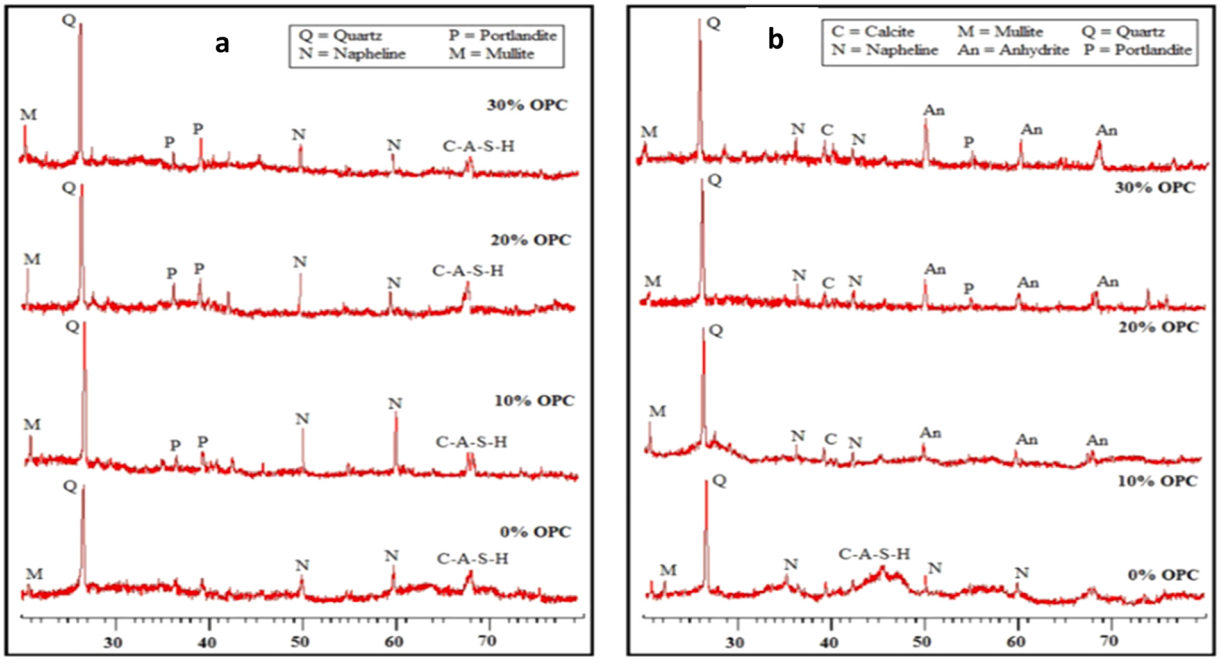

Fig. 12. a and b. is for unexposed sample and for sample exposed to the sulfuric acid solution for 365 days.
Reproduced with permission [57].

new peaks, anhydrite, and calcite after being subjected to sulphuric acid for 365 days. Anhydrite is calcium sulfate, which forms in the OGPC-blended geopolymer system due to the interaction between sulfuric acid and calcium-based hydrated products, whereas calcite is calcium carbonate [67,96]. The peak intensities of anhydrite and calcite rose as the OGPC concentration increased. Calcium sulfate production had a detrimental influence on the CS of exposed specimens and can be considered a significant component of concrete degradation.

The application of external load causes concrete to collapse more quickly and deteriorate. Previous investigations have also revealed similar degradation owing to calcium sulfate layer formation [67,96,117].

22.3. Fourier-transform infrared spectroscopy (FTIR)

The strong signals were seen in GPC1.5(FA), and GPC1.5(OPC) samples at 3347 and 3488 cm^{-1} correspond to symmetric stretching vibrations of H-O groups in water molecules and Mg molecules, respectively $(-OH)_2$. Small bands on the GPC1.5(FA), spectrum at 2816 and 2882 cm^{-1} are ascribed to -CH groups, suggesting the presence of organic molecules from FA [2,96]. Stretching and bending vibrations of O-H bonds, showing the water molecules associated to the geopolymer network, are also ascribed to the bands situated at an interval of 1637–1793 cm^{-1}. The separation of absorption bands in the 1446–1476 cm^{-1} and 1422–1482 cm^{-1} ranges seen on GPC1.5(FA), and GPC1.5(OPC) samples, respectively, is connected. The C-O stretching of carbonate groups caused by unreacted Na^+ during the Geopolymerization process with atmospheric air CO_2 is known as the efflorescence phenomenon [19,101,116,117]. According to a previous study, the degree of splitting is determined by the metal cation type that can fix the carbonate group. The chemical makeup of both solid precursor materials included Mg, Na, Fe, and Ca oxides. In an alkaline medium, these oxides would release Mg^{2+}, Na^+, Fe^{2+}/Fe^{3+}, and Ca^{2+} ions, which might be linked to CO_2. However, despite the presence of other ions, Ca^{2+} and Na^+ ions are responsible for the degree of splitting (seen on FTIR spectra in Fig. 13). The symmetric and asymmetric vibrations of the Si-O-T (T = Al or Si) bond connected to the geopolymer network are linked to absorption bands emerging at 1039 and 1087 cm^{-1} in both geopolymer concrete specimens[53,100]. These values are greater than those reported in the literature (about 1000 cm^{-1}), which might be attributed to calcium ions inserted into the tetrahedra site or different silica species from silica sources resulting in a geopolymer network expansion [81]. The stretching vibration of the 6-coordinated Al (VI)-O bond is responsible for the band at 777 cm in all spectra [87,89,126].

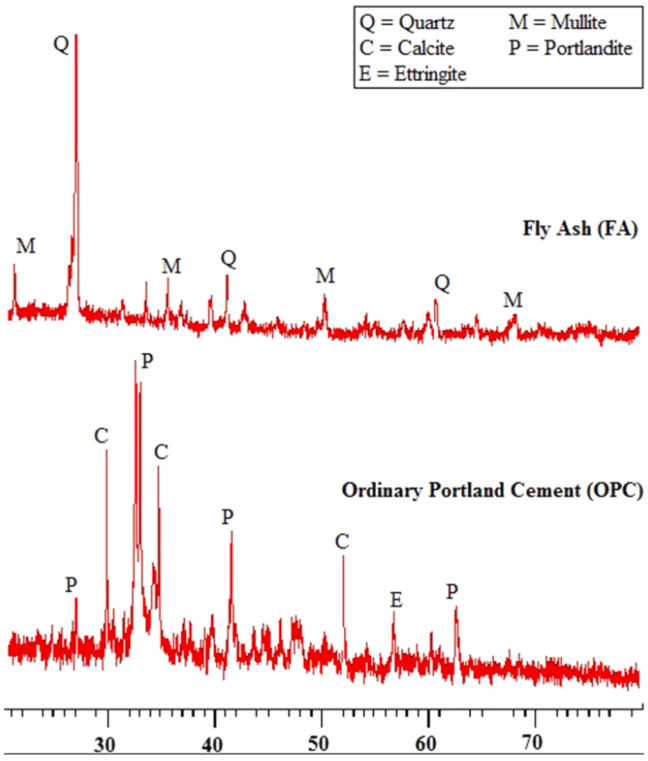

Fig. 13. Shows the FTIR spectra of GPC1.5(FA) and GPC1.5(OPC) samples.
Reproduced with permission [57].

23. Practical application of geopolymer materials

23.1. Geopolymer mortar

In general, the geopolymerization reaction is accelerated when the temperature is greater than ambient. At ambient curing, fly ash-based geopolymer mortar has lower compressive strength and more drying shrinkage than heat curing [122]. As a result, researchers used enhanced curing at high temperatures, which ranged from 40 to 90 °C. Although researchers have reported that heat cured geopolymer mortar can achieve CS of over 60 MPa, resistance to aggressive acids, sulphate attacks, good bond strength, and resistance to elevated temperatures, the need for an expensive and robust heat curing mechanism limits their use to the precast industry [115]. The magnitude of the temperature-dependent geopolymerization reaction has a substantial impact on the microstructure and mechanical characteristics of the geopolymer matrix. Mechanical characteristics of metakaolin mixed GPM improved significantly. Metakaolin's tiny particle size acts as a micro-aggregate, filling the pores and reducing porosity and densifying the microstructure [62]. The addition of nano-silica to GPM and concrete resulted in more nanoparticles and a larger surface area, requiring more water, and reducing workability. The addition of nano-silica improves the rate of dissolution of the silica and alumina phases, as well as the rate of polymerization, which improves the mechanical strength and durability qualities when cured at room temperature [26]. The use of Alccofine boosts the production of CSH and geopolymer gel, resulting in a higher CS and longer lasting product [127].

24. Self compacting geopolymer concrete (SCGC)

Ordinary geopolymer concrete requires vibratory compaction to provide good compactability. Noise pollution is aided by the vibration of concrete. It can be replaced with self-compacting concrete (SCC), which does not require any compacting and fills every corner of the formwork under its own weight [128].

SCC has benefits such as simple concrete filling in narrow and limited sections, increased compaction, strong bond strength with reinforcement, decreased maintenance, quick rate of construction, enhanced concrete quality, and lower total construction costs. Silica fume, FA, and GGBFS are commonly used in the construction of high strength-high performance concrete because to their excellent engineering qualities [41]. The advantages of geopolymer technology, as well as the growing tendency in the building industry toward SCC, drive the development of new concrete that combines the advantages of both forms of concrete. SCGC development does not necessitate any type of compaction and does not require the use of Portland cement [128,129]. SCGC has been researched by a limited number of researchers. Memon et al. produced SCGC utilizing FA as a source material by adjusting the sodium hydroxide molarity, sodium silicate to sodium hydroxide ratio, curing temperature, curing time, superplasticizer dose, and percentage of alkaline activator under temperature curing in a series of studies [130]. At ambient temperature, the compressive strength of GGBS-based SCGC was 40 MPa after 56 days, but the compressive strength of FA-based SCGC was only 16 MPa [131].

25. Geopolymer brick

Geopolymer bricks are a recent development in the brick business. The raw material for geopolymer bricks is fly ash, and the polymerization reaction is activated by an alkaline activator. The CS value of GGBS-developed bricks is greater than that of clay bricks. The GGBS was fully mixed with hydrated lime and sand, and brick specimens were crushed in a hydraulic machine at a pressure of 4.9 MPa [124]. The bricks were evaluated for CS for saturated circumstances, water absorption characteristics, and bulk density after 28 days of curing at 270–272 °C and 95% humidity. The authors came to the conclusion that a slag-lime, sand, and combination may be used to make noble grade bricks [106]. The brick was made with varied quantities of GGBS and sand as basic ingredients. The brick moulds were compacted at a pressure of 20 MPa, and they were evaluated for CS and freeze-thaw durability [108]. FA-based geopolymer bricks made with NaOH and Na_2SiO_3 outperform clay brick in terms of structural performance. The studies performed on a polymeric matrix with soluble silicate binders of varied degrees reveal encouraging results. The author evaluated the durability and CS properties of lightweight concrete blocks. Bricks may be made from industrial and agricultural wastes such as rice husk ash and expanded polystyrene [124]. Lime, gypsum, and diatomaceous earth lightweight bricks have better mechanical and thermal qualities. The gold mill waste materials were mixed with cement to make bricks. The cement-tailings bricks were cured by immersing them in water for various periods of time, and their CS was determined. Up to 20% of tailing was replaced with cement, and after 14 days of curing, the results were good [1,61,106].

26. Sustainable repair material

The use of Geopolymer binder has been widely researched due to its low shrinkage, high early strength, resistance to sulphate attack and corrosion, and good thawing and freezing resistance [83]. It may substantially reduce stripping time, speed up the template operation cycle, and enhance building speed when used in civil engineering. One-part GP mixes are a novel form of geopolymer binders that may be employed to make the activation of GPs in silicate solution easier [65]. Thermal treatment of low-quality kaolin at 950 °C increases the strength of the matching binders by up to 47 MP. Two-part mix systems might provide equivalent strength. Because of its acid resistance, high mechanical strength, longevity, and low permeability, Geopolymer cement is suited for storage wells under deep down-hole stress conditions for carbon capture [113]. Geopolymer cement is being considered as a possible portland cement substitute. This is mostly based on the features and requirements for sustainability [12].

27. Issue associated with geopolymer concrete

Geopolymer concrete is an innovative material that may be utilized in transportation infrastructure, specific projects, and offshore structures instead of typical Portland concrete or cement. It is extremely resistant to a lot of the difficulties that cause standard concretes to fracture and crumble [125,131]. There is a serious issue with this matter in the case of Geopolymer compounds in particular. It is occasionally required to apply superplasticizers to address this attribute since the materials have a high viscosity and, as a result, inadequate workability parameters. However, researching the rheology and workability of building materials is extremely challenging [132].

Employing natural materials that have been little treated or industrial waste. Portland concrete takes longer to cure than geopolymer concrete. Within 24 hrs, they had gained the majority of their strength. Difficult to prepare the geopolymer concrete, which is incredibly difficult to make and requires specific handling. It necessitates the use of potentially relatively toxic chemicals, such as sodium hydroxide [133]. Due to the hazards connected with its manufacture, geopolymer concrete is only available as a pre-cast or pre-mix material. The Geopolymerization Process is sensitive, research in this sector has shown to be inconclusive and volatile. There is a lack of consistency. While the concept of geopolymer concrete appears to be great and might be the best thing to happen to concrete since Portland, there are still too many unstable concerns that can create huge snags in the mixing and application process [111]. There of possibilities and vast to explore to achieve required properties, however, it needs thorough research in scale up production of geopolymer, it will helpfully achieve the properties relatively as same traditional concrete.

28. Conclusion

The variation of results of mechanical properties of GPC was investigated by evaluating previously reported papers such as slump, CS, STS, FS, WA, and BD. The effect of different molarity ranging from (5, 8−20) M and A/B ratio ranging from (0.25–0.50) on mechanical properties of geopolymer was investigated. Mainly, slump values decreased with the increase in the molar concentration. As the CS, STS, FS values for 7, 14, and 28 days increase with a molar concentration. In that, at 16–18 M, maximum CS, STS, and FS values were observed. The A/B ratio of 0.35, maximum STS and FS were observed. WA and BD increase with the intensification in A/B ratio up to 0.4 and 0.5, respectively. Various controlling factor on which performances of GPC depends is the molarity of activator, A/B ratio, SS/SH ratio, type of binder material selected for polymerization, size, shape, the physical and chemical composition of the binder, curing condition.

The maximum strength for mechanical properties for molarity was in the range of 16–18 M but depending upon the molarity changes above controlling factor. The addition of an activator agent could increase the Si/Al ratio. The ratio Si/Al in the range of 2–3 in the total matrix of GPC can be attained from different combinations of binder (material rich in Si and Al) or activator that enhances better structural performances of GPC. Industrial waste rich in Si and Al acts as a better binder in GPC. The increase in the amount of reactive particles proposes a fusion of the alkali resulting in Physico-chemical changes such as the disruption of crystalline phases and proclamation of silica and alumina, which leads to an increase in the reactivity in the polymerization process. Activator with high molarity improves accelerate the polycondensation leading to the rapid rate of chemical reaction in the polymer matrix.

Declaration of Competing Interest

The authors declare that they have no known competing financial interests or personal relationships that could have appeared to influence the work reported in this paper.

Acknowledgments

The author extends his appreciation to the Deanship of Scientific Research at King Khalid University, Saudi Arabia, for funding this work through research groups program under grant number (R.G.P. 1/248/42).

References

[1] I. Garcia-Lodeiro, A. Palomo, A. Fernández-Jiménez, 2 - An overview of the chemistry of alkali-activated cement-based binders, in: F. Pacheco-Torgal, J. A. Labrincha, C. Leonelli, A. Palomo, P. Chindaprasirt (Eds.), Handbook of Alkali-Activated Cements, Mortars and Concretes, Woodhead Publishing, Oxford, 2015, pp. 19–47, https://doi.org/10.1533/9781782422884.1.19.

[2] B. Mendes, I.K. Andrade, J.M. de Carvalho, L. Pedroti, A. de, O. Júnior, Assessment of mechanical and microstructural properties of geopolymers produced from metakaolin, silica fume, and red mud, Int. J. Appl. Ceram. Technol. 18 (2021) 262–274, https://doi.org/10.1111/ijac.13635.

[3] J.L. Provis, A. Palomo, C. Shi, Advances in understanding alkali-activated materials, Cem. Concr. Res. 78 (2015) 110–125, https://doi.org/10.1016/j.cemconres.2015.04.013.

[4] S. Ali, M.N. Sheikh, M.N.S. Hadi, Behavior of axially loaded plain and fiber-reinforced geopolymer concrete columns with glass fiber-reinforced polymer cages, Structural Concrete. n/a (n.d.). ⟨https://doi.org/10.1002/suco.202000231⟩.

[5] A. Hassan, M. Arif, M. Shariq, Age-dependent compressive strength and elastic modulus of fly ash-based geopolymer concrete, Structural Concrete. n/a (n.d.). ⟨https://doi.org/10.1002/suco.202000372⟩.

[6] M. Padmakar, B. Barhmaiah, M. Leela Priyanka, Characteristic compressive strength of a geo polymer concrete, Mater. Today. Proc. 37 (2021) 2219–2222, https://doi.org/10.1016/j.matpr.2020.07.656.

[7] K. Bakthavatchalam, M. Rajendran, An experimental investigation on potassium activator based geopolymer concrete incorporated with hybrid fibers, Mater. Today. Proc. (2021), https://doi.org/10.1016/j.matpr.2021.03.506.

[8] G. Jayarajan, S. Arivalagan, An experimental studies of geopolymer concrete incorporated with fly-ash & GGBS, Mater. Today. Proc. (2021), https://doi.org/10.1016/j.matpr.2021.01.285.

[9] S.K. Das, J. Mishra, S.K. Singh, S.M. Mustakim, A. Patel, S.K. Das, U. Behera, Characterization and utilization of rice husk ash (RHA) in fly ash – Blast furnace slag based geopolymer concrete for sustainable future, Mater. Today. Proc. 33 (2020) 5162–5167, https://doi.org/10.1016/j.matpr.2020.02.870.

[10] S.K. Das, S. Shrivastava, Siliceous fly ash and blast furnace slag based geopolymer concrete under ambient temperature curing condition, Struct. Concr. 22 (2021) E341–E351, https://doi.org/10.1002/suco.201900201.

[11] W.K.W. Lee, J.S.J. van Deventer, Chemical interactions between siliceous aggregates and low-Ca alkali-activated cements, Cem. Concr. Res. 37 (2007) 844–855, https://doi.org/10.1016/j.cemconres.2007.03.012.

[12] Y.H.M. Amran, R. Alyousef, H. Alabduljabbar, M. El-Zeadani, Clean production and properties of geopolymer concrete: a review, J. Clean. Prod. 251 (2020), 119679, https://doi.org/10.1016/j.jclepro.2019.119679.

[13] P. Chindaprasirt, C. Jaturapitakkul, W. Chalee, U. Rattanasak, Comparative study on the characteristics of fly ash and bottom ash geopolymers, Waste Manag. 29 (2009) 539–543, https://doi.org/10.1016/j.wasman.2008.06.023.

[14] G.F. Huseien, M. Ismail, N.H.A. Khalid, M.W. Hussin, J. Mirza, Compressive strength and microstructure of assorted wastes incorporated geopolymer mortars: effect of solution molarity, Alex. Eng. J. 57 (2018) 3375–3386, https://doi.org/10.1016/j.aej.2018.07.011.

[15] J. Xie, W. Chen, J. Wang, C. Fang, B. Zhang, F. Liu, Coupling effects of recycled aggregate and GGBS/metakaolin on physicochemical properties of geopolymer concrete, Constr. Build. Mater. 226 (2019) 345–359, https://doi.org/10.1016/j.conbuildmat.2019.07.311.

[16] C.R. Meesala, N.K. Verma, S. Kumar, Critical review on fly-ash based geopolymer concrete, Struct. Concr. 21 (2020) 1013–1028, https://doi.org/10.1002/suco.201900326.

[17] D.M.A. Huiskes, A. Keulen, Q.L. Yu, H.J.H. Brouwers, Design and performance evaluation of ultra-lightweight geopolymer concrete, Mater. Des. 89 (2016) 516–526, https://doi.org/10.1016/j.matdes.2015.09.167.

[18] J.M. Their, M. Özakça, Developing geopolymer concrete by using cold-bonded fly ash aggregate, nano-silica, and steel fiber, Constr. Build. Mater. 180 (2018) 12–22, https://doi.org/10.1016/j.conbuildmat.2018.05.274.

[19] A.C. Ganesh, M. Muthukannan, Development of high performance sustainable optimized fiber reinforced geopolymer concrete and prediction of compressive strength, J. Clean. Prod. 282 (2021), 124543, https://doi.org/10.1016/j.jclepro.2020.124543.

[20] N. Ganesan, R. Abraham, S. Deepa Raj, Durability characteristics of steel fibre reinforced geopolymer concrete, Constr. Build. Mater. 93 (2015) 471–476, https://doi.org/10.1016/j.conbuildmat.2015.06.014.

[21] A. Krishna Rao, D.R. Kumar, Effect of various alkaline binder ratio on geopolymer concrete under ambient curing condition, Mater. Today. Proc. 27 (2020) 1768–1773, https://doi.org/10.1016/j.matpr.2020.03.682.

[22] J. Zhang, C. Shi, Z. Zhang, Z. Ou, Durability of alkali-activated materials in aggressive environments: a review on recent studies, Constr. Build. Mater. 152 (2017) 598–613, https://doi.org/10.1016/j.conbuildmat.2017.07.027.

[23] A.R.G. de Azevedo, M.T. Marvila, L.B. de Oliveira, W.M. Ferreira, H. Colorado, S.R. Teixeira, C.M.F. Vieira, Circular economy and durability in geopolymers ceramics pieces obtained from glass polishing waste, International Journal of Applied Ceramic Technology. n/a (n.d.). ⟨https://doi.org/10.1111/ijac.13780⟩.

[24] F.N. Okoye, S. Prakash, N.B. Singh, Durability of fly ash based geopolymer concrete in the presence of silica fume, J. Clean. Prod. 149 (2017) 1062–1067, https://doi.org/10.1016/j.jclepro.2017.02.176.

[25] K. Pasupathy, M. Berndt, J. Sanjayan, P. Rajeev, D.S. Cheema, Durability of low-calcium fly ash based geopolymer concrete culvert in a saline environment, Cem. Concr. Res. 100 (2017) 297–310, https://doi.org/10.1016/j.cemconres.2017.07.010.

[26] H.E. Elyamany, A.E.M. Abd Elmoaty, A.M. Elshaboury, Setting time and 7-day strength of geopolymer mortar with various binders, Constr. Build. Mater. 187 (2018) 974–983, https://doi.org/10.1016/j.conbuildmat.2018.08.025.

[27] Saloni Parveen, T.M. Pham, Y.Y. Lim, S.S. Pradhan, J.Kumar Jatin, Performance of rice husk ash-based sustainable geopolymer concrete with ultra-fine slag and Corn cob ash, Constr. Build. Mater. 279 (2021), 122526, https://doi.org/10.1016/j.conbuildmat.2021.122526.

[28] H. Sethi, P.P. Bansal, R. Sharma, Effect of addition of GGBS and glass powder on the properties of geopolymer concrete, Iran. J. Sci. Technol. Trans. Civ. Eng. 43 (2019) 607–617, https://doi.org/10.1007/s40996-018-0202-4.

[29] S.A. Bernal, R. Mejía de Gutiérrez, A.L. Pedraza, J.L. Provis, E.D. Rodriguez, S. Delvasto, Effect of binder content on the performance of alkali-activated slag concretes, Cem. Concr. Res. 41 (2011) 1–8, https://doi.org/10.1016/j.cemconres.2010.08.017.

[30] J. Davidovits, Geopolymer, Green Chemistry and Sustainable Development Solutions: Proceedings of the World Congress Geopolymer 2005, Geopolymer Institute, 2005.

[31] K.M.L. Alventosa, C.E. White, The effects of calcium hydroxide and activator chemistry on alkali-activated metakaolin pastes, Cem. Concr. Res. 145 (2021), 106453, https://doi.org/10.1016/j.cemconres.2021.106453.

[32] C.K. Yip, G.C. Lukey, J.L. Provis, J.S.J. van Deventer, Effect of calcium silicate sources on geopolymerisation, Cem. Concr. Res. 38 (2008) 554–564, https://doi.org/10.1016/j.cemconres.2007.11.001.

[33] Z. Luo, W. Li, K. Wang, A. Castel, S.P. Shah, Comparison on the properties of ITZs in fly ash-based geopolymer and Portland cement concretes with equivalent flowability, Cem. Concr. Res. 143 (2021), 106392, https://doi.org/10.1016/j.cemconres.2021.106392.

[34] H.U. Ahmed, A.A. Mohammed, A.S. Mohammed, The role of nanomaterials in geopolymer concrete composites: a state-of-the-art review, J. Build. Eng. 49 (2022), 104062, https://doi.org/10.1016/j.jobe.2022.104062.

[35] S. Singh, M.U. Aswath, R.V. Ranganath, Effect of mechanical activation of red mud on the strength of geopolymer binder, Constr. Build. Mater. 177 (2018) 91–101, https://doi.org/10.1016/j.conbuildmat.2018.05.096.

[36] H.U. Ahmed, A.A. Mohammed, S. Rafiq, A.S. Mohammed, A. Mosavi, N.H. Sor, S.M.A. Qaidi, Compressive strength of sustainable geopolymer concrete composites: a state-of-the-art review, Sustainability 13 (2021) 13502, https://doi.org/10.3390/su132413502.

[37] S.J. Chithambaram, S. Kumar, M.M. Prasad, D. Adak, Effect of parameters on the compressive strength of fly ash based geopolymer concrete, Struct. Concr. 19 (2018) 1202–1209, https://doi.org/10.1002/suco.201700235.

[38] F.N. Okoye, J. Durgaprasad, N.B. Singh, Effect of silica fume on the mechanical properties of fly ash based-geopolymer concrete, Ceram. Int. 42 (2016) 3000–3006, https://doi.org/10.1016/j.ceramint.2015.10.084.

[39] J. Davidovits , Geopolymers Based on Natural and Synthetic Metakaolin a Critical Review 2018 , in: Proceedings of the 41st International Conference on Advanced Ceramics and Composites, John Wiley & Sons, Ltd, 201 214 doi: 10.1002/9781119474746.ch19.in: Proceedings of the 41st International Conference on Advanced Ceramics and Composites.

[40] P. Chindaprasirt, W. Chalee, Effect of sodium hydroxide concentration on chloride penetration and steel corrosion of fly ash-based geopolymer concrete under marine site, Constr. Build. Mater. 63 (2014) 303–310, https://doi.org/10.1016/j.conbuildmat.2014.04.010.

[41] N.V. K, D.L.V. Babu, Assessing the performance of molarity and alkaline activator ratio on engineering properties of self-compacting alkaline activated concrete at ambient temperature, J. Build. Eng. 20 (2018) 137–155, https://doi.org/10.1016/j.jobe.2018.07.005.

[42] İ.B. Topçu, M.U. Toprak, T. Uygunoğlu, Durability and microstructure characteristics of alkali activated coal bottom ash geopolymer cement, J. Clean. Prod. 81 (2014) 211–217, https://doi.org/10.1016/j.jclepro.2014.06.037.

[43] M. Zerzouri, O. Bouchenafa, R. Hamzaoui, L. Ziyani, S. Alehyen, Physico-chemical and mechanical properties of fly ash based-geopolymer pastes produced from pre-geopolymer powders obtained by mechanosynthesis, Constr. Build. Mater. 288 (2021), 123135, https://doi.org/10.1016/j.conbuildmat.2021.123135.

[44] S. Haruna, B.S. Mohammed, M.M.A. Wahab, M.S. Liew, Effect of paste aggregate ratio and curing methods on the performance of one-part alkali-activated concrete, Constr. Build. Mater. 261 (2020) (accessed October 24, 2021).

[45] M.M. Al Bakri Abdullah, H. Kamarudin, O.A.K.A. Abdulkareem, C.M.R. Ghazali, A.R. Rafiza, M.N. Norazian, Optimization of alkaline activator/fly ash ratio on the compressive strength of manufacturing fly ASH-BASED geopolymer, Appl. Mech. Mater. 110–116 (2012) 734–739, https://doi.org/10.4028/www.scientific.net/AMM.110-116.734.

[46] M.T. Ghafoor, Q.S. Khan, A.U. Qazi, M.N. Sheikh, M.N.S. Hadi, Influence of alkaline activators on the mechanical properties of fly ash based geopolymer concrete cured at ambient temperature, Constr. Build. Mater. 273 (2021), 121752, https://doi.org/10.1016/j.conbuildmat.2020.121752.

[47] M. Koushkbaghi, P. Alipour, B. Tahmouresi, E. Mohseni, A. Saradar, P.K. Sarker, Influence of different monomer ratios and recycled concrete aggregate on mechanical properties and durability of geopolymer concretes, Constr. Build. Mater. 205 (2019) 519–528, https://doi.org/10.1016/j.conbuildmat.2019.01.174.

[48] K.K. Poloju, K. Sinivasu, Influence of GGBS and alkaline ratio on compression strength of geopolymer concrete: influence of GGBS and alkaline ratio on compression strength of geopolymer concrete, SPAST Abstr. 1 (2021) (accessed November 5, 2021).

[49] M.E.L. Alouani, S. Alehyen, M.E.L. Achouri, A. Hajjaji, C. Ennawaoui, M. Taibi, Influence of the nature and rate of alkaline activator on the physicochemical properties of fly ash-based geopolymers, Adv. Civ. Eng. 2020 (2020), e8880906, https://doi.org/10.1155/2020/8880906.

[50] H.U. Ahmed, A.S. Mohammed, A.A. Mohammed, R.H. Faraj, Systematic multiscale models to predict the compressive strength of fly ash-based geopolymer concrete at various mixture proportions and curing regimes, PLOS ONE 16 (2021), e0253006, https://doi.org/10.1371/journal.pone.0253006.

[51] A.E. Kurtoglu, R. Alzeebaree, O. Aljumaili, A. Nis, M.E. Gulsan, G. Humur, A. Cevik, Mechanical and durability properties of fly ash and slag based geopolymer concrete, 1. 6 (2018) 345–362. (accessed April 29, 2021).

[52] P. Palanisamy, P.S. Kumar, Effect of molarity in geo polymer earth brick reinforced with fibrous coir wastes using sandy soil and quarry dust as fine aggregate. (Case study), Case Stud. Constr. Mater. 8 (2018) 347–358, https://doi.org/10.1016/j.cscm.2018.01.009.

[53] M.L.Y. Yeoh, S. Ukritnukun, A. Rawal, J. Davies, B.J. Kang, K. Burrough, Z. Aly, P. Dayal, E.R. Vance, D.J. Gregg, P. Koshy, C.C. Sorrell, Mechanistic impacts of long-term gamma irradiation on physicochemical, structural, and mechanical stabilities of radiation-responsive geopolymer pastes, J. Hazard. Mater. 407 (2021), 124805, https://doi.org/10.1016/j.jhazmat.2020.124805.

[54] X. Liang, Y. Ji, Mechanical properties and permeability of red mud-blast furnace slag-based geopolymer concrete, SN Appl. Sci. 3 (2021) 23, https://doi.org/10.1007/s42452-020-03985-4.

[55] A. Hajimohammadi, J.L. Provis, J.S.J. van Deventer, The effect of silica availability on the mechanism of geopolymerisation, Cem. Concr. Res. 41 (2011) 210–216, https://doi.org/10.1016/j.cemconres.2011.02.001.

[56] S. Hanjitsuwan, S. Hunpratub, P. Thongbai, S. Maensiri, V. Sata, P. Chindaprasirt, Effects of NaOH concentrations on physical and electrical properties of high calcium fly ash geopolymer paste, Cem. Concr. Compos. 45 (2014) 9–14, https://doi.org/10.1016/j.cemconcomp.2013.09.012.

[57] A. Mehta, R. Siddique, Sulfuric acid resistance of fly ash based geopolymer concrete, Constr. Build. Mater. 146 (2017) 136–143, https://doi.org/10.1016/j.conbuildmat.2017.04.077.

[58] A. Hassan, M. Arif, M. Shariq, Use of geopolymer concrete for a cleaner and sustainable environment – a review of mechanical properties and microstructure, J. Clean. Prod. 223 (2019) 704–728, https://doi.org/10.1016/j.jclepro.2019.03.051.

[59] K. Bakthavatchalam, M. Rajendran, An experimental investigation on potassium activator based geopolymer concrete incorporated with hybrid fibers, Mater. Today. Proc. (2021), https://doi.org/10.1016/j.matpr.2021.03.506.

[60] M. Amran, S. Debbarma, T. Ozbakkaloglu, Fly ash-based eco-friendly geopolymer concrete: a critical review of the long-term durability properties, Constr. Build. Mater. 270 (2021), 121857, https://doi.org/10.1016/j.conbuildmat.2020.121857.

[61] A. Palomo, O. Maltseva, I. Garcia-Lodeiro, A. Fernández-Jiménez, Portland versus alkaline cement: continuity or clean break: “a key decision for global sustainability, Front. Chem. 9 (2021) 653, https://doi.org/10.3389/fchem.2021.705475.

[62] A.B. Malkawi, M.F. Nuruddin, A. Fauzi, H. Almattarneh, B.S. Mohammed, Effects of alkaline solution on properties of the HCFA geopolymer mortars, Procedia Eng. 148 (2016) 710–717, https://doi.org/10.1016/j.proeng.2016.06.581.

[63] S. Bhattacherjee, A.S. Basavaraj, A.V. Rahul, M. Santhanam, R. Gettu, B. Panda, E. Schlangen, Y. Chen, O. Copuroglu, G. Ma, L. Wang, M.A. Basit Beigh, V. Mechtcherine, Sustainable materials for 3D concrete printing, Cem. Concr. Compos. 122 (2021), 104156, https://doi.org/10.1016/j.cemconcomp.2021.104156.

[64] P.Y. He, Y.J. Zhang, H. Chen, L.C. Liu, Development of an eco-efficient CaMoO4/electroconductive geopolymer composite for recycling silicomanganese slag and degradation of dye wastewater, J. Clean. Prod. 208 (2019) 1476–1487, https://doi.org/10.1016/j.jclepro.2018.10.176.

[65] A.Z. Khalifa, Ö. Cizer, Y. Pontikes, A. Heath, P. Patureau, S.A. Bernal, A.T.M. Marsh, Advances in alkali-activation of clay minerals, Cem. Concr. Res. 132 (2020), 106050, https://doi.org/10.1016/j.cemconres.2020.106050.

[66] E. Álvarez-Ayuso, X. Querol, F. Plana, A. Alastuey, N. Moreno, M. Izquierdo, O. Font, T. Moreno, S. Diez, E. Vázquez, M. Barra, Environmental, physical and structural characterisation of geopolymer matrixes synthesised from coal (co-)combustion fly ashes, J. Hazard. Mater. 154 (2008) 175–183, https://doi.org/10.1016/j.jhazmat.2007.10.008.

[67] A. Bouaissi, L. Li, M.M. Al Bakri Abdullah, Q.-B. Bui, Mechanical properties and microstructure analysis of FA-GGBS-HMNS based geopolymer concrete, Constr. Build. Mater. 210 (2019) 198–209, https://doi.org/10.1016/j.conbuildmat.2019.03.202.

[68] Y. Hu, Z. Tang, W. Li, Y. Li, V.W.Y. Tam, Physical-mechanical properties of fly ash/GGBFS geopolymer composites with recycled aggregates, Constr. Build. Mater. 226 (2019) 139–151, https://doi.org/10.1016/j.conbuildmat.2019.07.211.

[69] S. Luhar, S. Chaudhary, I. Luhar, Development of rubberized geopolymer concrete: strength and durability studies, Constr. Build. Mater. 204 (2019) 740–753, https://doi.org/10.1016/j.conbuildmat.2019.01.185.

[70] S. Naskar, A.K. Chakraborty, Effect of nano materials in geopolymer concrete, Perspect. Sci. 8 (2016) 273–275, https://doi.org/10.1016/j.pisc.2016.04.049.

[71] D. Adak, M. Sarkar, S. Mandal, Effect of nano-silica on strength and durability of fly ash based geopolymer mortar, Constr. Build. Mater. 70 (2014) 453–459, https://doi.org/10.1016/j.conbuildmat.2014.07.093.

[72] A.A. Aliabdo, A.E.M. Abd Elmoaty, H.A. Salem, Effect of water addition, plasticizer and alkaline solution constitution on fly ash based geopolymer concrete performance, Constr. Build. Mater. 121 (2016) 694–703, https://doi.org/10.1016/j.conbuildmat.2016.06.062.

[73] A.A. Shahmansouri, H. Akbarzadeh Bengar, S. Ghanbari, Compressive strength prediction of eco-efficient GGBS-based geopolymer concrete using GEP method, J. Build. Eng. 31 (2020), 101326, https://doi.org/10.1016/j.jobe.2020.101326.

[74] D. Ravikumar, N. Neithalath, Effects of activator characteristics on the reaction product formation in slag binders activated using alkali silicate powder and NaOH, Cem. Concr. Compos. 34 (2012) 809–818, https://doi.org/10.1016/j.cemconcomp.2012.03.006.

[75] S.H.G. Mousavinejad, M.F. Gashti, Effects of alkaline solution/binder and Na2SiO3/NaOH ratios on fracture properties and ductility of ambient-cured GGBFS based heavyweight geopolymer concrete, Structures 32 (2021) 2118–2129, https://doi.org/10.1016/j.istruc.2021.04.008.

[76] M. Sofi, J.S.J. van Deventer, P.A. Mendis, G.C. Lukey, Engineering properties of inorganic polymer concretes (IPCs), Cem. Concr. Res. 37 (2007) 251–257, https://doi.org/10.1016/j.cemconres.2006.10.008.

[77] K. Pasupathy, J. Sanjayan, P. Rajeev, Evaluation of alkalinity changes and carbonation of geopolymer concrete exposed to wetting and drying, J. Build. Eng. 35 (2021), 102029, https://doi.org/10.1016/j.jobe.2020.102029.

[78] M. Verma, N. Dev, Sodium hydroxide effect on the mechanical properties of flyash-slag based geopolymer concrete, Struct. Concr. 22 (2021) E368–E379, https://doi.org/10.1002/suco.202000068.

[79] P. Chindaprasirt, T. Chareerat, V. Sirivivatnanon, Workability and strength of coarse high calcium fly ash geopolymer, Cem. Concr. Compos. 29 (2007) 224–229, https://doi.org/10.1016/j.cemconcomp.2006.11.002.

[80] G.S. Ryu, Y.B. Lee, K.T. Koh, Y.S. Chung, The mechanical properties of fly ash-based geopolymer concrete with alkaline activators, Constr. Build. Mater. 47 (2013) 409–418, https://doi.org/10.1016/j.conbuildmat.2013.05.069.

[81] Improvement in Fresh, Mechanical and Microstructural Properties of Fly Ash- Blast Furnace Slag Based Geopolymer Concrete By Addition of Nano and Micro Silica | SpringerLink, (n.d.). ⟨https://link.springer.com/article/10.1007/s12633–020-00593–0⟩ (accessed June 12, 2021).

[82] M. Alghannam, A. Albidah, H. Abbas, Y. Al-Salloum, Influence of critical parameters of mix proportions on properties of MK-based geopolymer concrete, Arab J. Sci. Eng. 46 (2021) 4399–4408, https://doi.org/10.1007/s13369-020-04970-0.

[83] A. Mehta, R. Siddique, Sustainable geopolymer concrete using ground granulated blast furnace slag and rice husk ash: strength and permeability properties, J. Clean. Prod. 205 (2018) 49–57, https://doi.org/10.1016/j.jclepro.2018.08.313.

[84] U. Durak, O. Karahan, B. Uzal, S. İlkentapar, C.D. Atiş, Influence of nano SiO2 and nano CaCO3 particles on strength, workability, and microstructural properties of fly ash-based geopolymer, Struct. Concr. 22 (2021) E352–E367, https://doi.org/10.1002/suco.201900479.

[85] K. Gao, K.-L. Lin, D. Wang, H.-S. Shiu, C.-L. Hwang, B.L.A. Tuan, T.-W. Cheng, Thin-film-transistor liquid-crystal display waste glass and nano-SiO2 as substitute sources for metakaolin-based geopolymer, Environ. Prog. Sustain. Energy 33 (2014) 947–955, https://doi.org/10.1002/ep.11868.

[86] F.N. Okoye, J. Durgaprasad, N.B. Singh, Mechanical properties of alkali activated flyash/Kaolin based geopolymer concrete, Constr. Build. Mater. 98 (2015) 685–691, https://doi.org/10.1016/j.conbuildmat.2015.08.009.

[87] A.M. Aly, M.S. El-Feky, M. Kohail, E.-S.A.R. Nasr, Performance of geopolymer concrete containing recycled rubber, Constr. Build. Mater. 207 (2019) 136–144, https://doi.org/10.1016/j.conbuildmat.2019.02.121.

[88] S. Mesgari, A. Akbarnezhad, J.Z. Xiao, Recycled geopolymer aggregates as coarse aggregates for Portland cement concrete and geopolymer concrete: Effects on mechanical properties, Constr. Build. Mater. 236 (2020), 117571, https://doi.org/10.1016/j.conbuildmat.2019.117571.

[89] M. Sarkar, K. Dana, Partial replacement of metakaolin with red ceramic waste in geopolymer, Ceram. Int. 47 (2021) 3473–3483, https://doi.org/10.1016/j.ceramint.2020.09.191.

[90] B.C. Mendes, L.G. Pedroti, C.M.F. Vieira, M. Marvila, A.R.G. Azevedo, J.M. Franco de Carvalho, J.C.L. Ribeiro, Application of eco-friendly alternative activators in alkali-activated materials: a review, J. Build. Eng. 35 (2021), 102010, https://doi.org/10.1016/j.jobe.2020.102010.

[91] A.R.G. de Azevedo, M.T. Marvila, M. Ali, M.I. Khan, F. Masood, C.M.F. Vieira, Effect of the addition and processing of glass polishing waste on the durability of geopolymeric mortars, Case Stud. Constr. Mater. 15 (2021), e00662, https://doi.org/10.1016/j.cscm.2021.e00662.

[92] P. Perez-Cortes, J.I. Escalante-Garcia, Gel composition and molecular structure of alkali-activated metakaolin-limestone cements, Cem. Concr. Res. 137 (2020), 106211, https://doi.org/10.1016/j.cemconres.2020.106211.

[93] D.B. Raijiwala, H.S. Patil, Geopolymer concrete A green concrete, in: 2010 2nd International Conference on Chemical, Biological and Environmental Engineering, 2010: pp. 202–206. ⟨https://doi.org/10.1109/ICBEE.2010.5649609⟩.

[95] P. Nath, P.K. Sarker, V.B. Rangan, Early age properties of low-calcium fly ash geopolymer concrete suitable for ambient Curing, Procedia Eng. 125 (2015) 601–607, https://doi.org/10.1016/j.proeng.2015.11.077.

[96] S. Pilehvar, V.D. Cao, A.M. Szczotok, L. Valentini, D. Salvioni, M. Magistri, R. Pamies, A.-L. Kjøniksen, Mechanical properties and microscale changes of geopolymer concrete and Portland cement concrete containing micro-encapsulated phase change materials, Cem. Concr. Res. 100 (2017) 341–349, https://doi.org/10.1016/j.cemconres.2017.07.012.

[97] J.S. Moya, B. Cabal, J. Sanz, R. Torrecillas, Metakaolin-nanosilver as biocide agent in geopolymer, in: Developments in Strategic Materials and Computational Design III, John Wiley & Sons, Ltd, 2012, pp. 1–11, https://doi.org/10.1002/9781118217542.ch1.

[99] T. Luukkonen, Z. Abdollahnejad, J. Yliniemi, P. Kinnunen, M. Illikainen, One-part alkali-activated materials: a review, Cem. Concr. Res. 103 (2018) 21–34, https://doi.org/10.1016/j.cemconres.2017.10.001.

[100] A.A. Siyal, M.R. Shamsuddin, S.H. Khahro, A. Low, M. Ayoub, Optimization of synthesis of geopolymer adsorbent for the effective removal of anionic surfactant from aqueous solution, J. Environ. Chem. Eng. 9 (2021), 104949, https://doi.org/10.1016/j.jece.2020.104949.

[101] P.R. Vora, U.V. Dave, Parametric studies on compressive strength of geopolymer concrete, Procedia Eng. 51 (2013) 210–219, https://doi.org/10.1016/j.proeng.2013.01.030.

[102] A. Hasnaoui, E. Ghorbel, G. Wardeh, Effect of Curing conditions on the performance of geopolymer concrete based on granulated blast furnace slag and metakaolin, J. Mater. Civ. Eng. 33 (2021), 04020501, https://doi.org/10.1061/(ASCE)MT.1943-5533.0003606.

[103] K. Kishore, N. Gupta, Mechanical characterization and assessment of composite geopolymer concrete, Mater. Today. Proc. 44 (2021) 58–62, https://doi.org/10.1016/j.matpr.2020.06.319.

[104] M. Kaya, F. Köksal, Effect of cement additive on physical and mechanical properties of high calcium fly ash geopolymer mortars, Struct. Concr. 22 (2021) E452–E465, https://doi.org/10.1002/suco.202000235.

[105] M. Muraleedharan, Y. Nadir, Factors affecting the mechanical properties and microstructure of geopolymers from red mud and granite waste powder: a review, Ceram. Int. 47 (2021) 13257–13279, https://doi.org/10.1016/j.ceramint.2021.02.009.

[106] P. Indhiradevi, P. Manikandan, K. Rajkumar, S. Logeswaran, A comparative study on usage of cowdung ash and wood ash as partial replacement in flyash brick, Mater. Today. Proc. 37 (2021) 1190–1194, https://doi.org/10.1016/j.matpr.2020.06.355.

[107] R.R. Lloyd, J.L. Provis, J.S.J. van Deventer, Pore solution composition and alkali diffusion in inorganic polymer cement, Cem. Concr. Res. 40 (2010) 1386–1392, https://doi.org/10.1016/j.cemconres.2010.04.008.

[108] S. Apithanyasai, N. Supakata, S. Papong, The potential of industrial waste: using foundry sand with fly ash and electric arc furnace slag for geopolymer brick production, Heliyon 6 (2020), e03697, https://doi.org/10.1016/j.heliyon.2020.e03697.

[109] V. Medri, E. Papa, M. Mazzocchi, L. Laghi, M. Morganti, J. Francisconi, E. Landi, Production and characterization of lightweight vermiculite/geopolymer-based panels, Mater. Des. 85 (2015) 266–274, https://doi.org/10.1016/j.matdes.2015.06.145.

[110] C. Shi, B. Qu, J.L. Provis, Recent progress in low-carbon binders, Cem. Concr. Res. 122 (2019) 227–250, https://doi.org/10.1016/j.cemconres.2019.05.009.

[111] K. Zerfu, J.J. Ekaputri, Review on alkali-activated fly ash based geopolymer concrete, Mater. Sci. Forum 841 (2016) 162–169, https://doi.org/10.4028/www.scientific.net/MSF.841.162.

[112] Y. Qin, X. Chen, B. Li, Y. Guo, Z. Niu, T. Xia, W. Meng, M. Zhou, Study on the mechanical properties and microstructure of chitosan reinforced metakaolin-based geopolymer, Constr. Build. Mater. 271 (2021), 121522, https://doi.org/10.1016/j.conbuildmat.2020.121522.

[113] C.-K. Ma, A.Z. Awang, W. Omar, Structural and material performance of geopolymer concrete: a review, Constr. Build. Mater. 186 (2018) 90–102, https://doi.org/10.1016/j.conbuildmat.2018.07.111.

[114] S. Riahi, A. Nemati, A.R. Khodabandeh, S. Baghshahi, The effect of mixing molar ratios and sand particles on microstructure and mechanical properties of metakaolin-based geopolymers, Mater. Chem. Phys. 240 (2020), 122223, https://doi.org/10.1016/j.matchemphys.2019.122223.

[115] G. Görhan, G. Kürklü, The influence of the NaOH solution on the properties of the fly ash-based geopolymer mortar cured at different temperatures, Compos. Part B Eng. 58 (2014) 371–377, https://doi.org/10.1016/j.compositesb.2013.10.082.

[116] P. Duxson, J.L. Provis, G.C. Lukey, J.S.J. van Deventer, The role of inorganic polymer technology in the development of 'green concrete, Cem. Concr. Res. 37 (2007) 1590–1597, https://doi.org/10.1016/j.cemconres.2007.08.018.

[117] L.N. Assi, E. Eddie Deaver, P. Ziehl, Effect of source and particle size distribution on the mechanical and microstructural properties of fly Ash-Based geopolymer concrete, Constr. Build. Mater. 167 (2018) 372–380, https://doi.org/10.1016/j.conbuildmat.2018.01.193.

[118] M.T. Marvila, A.R.G. de Azevedo, P.R. de Matos, S.N. Monteiro, C.M.F. Vieira, Materials for production of high and ultra-high performance concrete: review and perspective of possible novel materials, Materials 14 (2021) 4304, https://doi.org/10.3390/ma14154304.

[119] Polymers | Free Full-Text | Natural Fibers as an Alternative to Synthetic Fibers in Reinforcement of Geopolymer Matrices: A Comparative Review | HTML, (n.d.). (accessed March 7, 2022).

[120] Experimental Investigations and Prediction of Thermal Behaviour of Ferrosialate-Based Geopolymer Mortars | SpringerLink, (n.d.). ⟨https://link.springer.com/article/10.1007/s13369–019-04314–7⟩ (accessed March 7, 2022).

[121] M.T. Marvila, A.R.G. Azevedo, G.C.G. Delaqua, B.C. Mendes, L.G. Pedroti, C.M.F. Vieira, Performance of geopolymer tiles in high temperature and saturation conditions, Constr. Build. Mater. 286 (2021), 122994, https://doi.org/10.1016/j.conbuildmat.2021.122994.

[122] G.F. Huseien, H.K. Hamzah, A.R. Mohd Sam, N.H.A. Khalid, K.W. Shah, D.P. Deogrescu, J. Mirza, Alkali-activated mortars blended with glass bottle waste nano powder: environmental benefit and sustainability, J. Clean. Prod. 243 (2020), 118636, https://doi.org/10.1016/j.jclepro.2019.118636.

[123] P. Nuaklong, A. Wongsa, K. Boonserm, C. Ngohpok, P. Jongvivatsakul, V. Sata, P. Sukontasukkul, P. Chindaprasirt, Enhancement of mechanical properties of fly ash geopolymer containing fine recycled concrete aggregate with micro carbon fiber, J. Build. Eng. 41 (2021), 102403, https://doi.org/10.1016/j.jobe.2021.102403.

[124] A. Wongsa, V. Sata, P. Nuaklong, P. Chindaprasirt, Use of crushed clay brick and pumice aggregates in lightweight geopolymer concrete, Constr. Build. Mater. 188 (2018) 1025–1034, https://doi.org/10.1016/j.conbuildmat.2018.08.176.

[125] H.K. Shehab, A.S. Eisa, A.M. Wahba, Mechanical properties of fly ash based geopolymer concrete with full and partial cement replacement, Constr. Build. Mater. 126 (2016) 560–565, https://doi.org/10.1016/j.conbuildmat.2016.09.059.

[126] Saloni Parveen, T.M. Pham, Y.Y. Lim, S.S. Pradhan, J.Kumar Jatin, Performance of rice husk Ash-Based sustainable geopolymer concrete with ultra-fine slag and Corn cob ash, Constr. Build. Mater. 279 (2021), 122526, https://doi.org/10.1016/j.conbuildmat.2021.122526.
[127] B.B. Jindal, Investigations on the properties of geopolymer mortar and concrete with mineral admixtures: a review, Constr. Build. Mater. 227 (2019), 116644, https://doi.org/10.1016/j.conbuildmat.2019.08.025.
[128] E. Kamseu, C. Ponzoni, C. Tippayasam, R. Taurino, D. Chaysuwan, V.M. Sglavo, P. Thavorniti, C. Leonelli, Self-compacting geopolymer concretes: effects of addition of aluminosilicate-rich fines, J. Build. Eng. 5 (2016) 211–221, https://doi.org/10.1016/j.jobe.2016.01.004.
[129] Development of self-compacting geopolymer concrete as a sustainable construction material - ScienceDirect, (n.d.)(Accessed 7 March 2022).
[130] Shear-bond behavior of self-compacting geopolymer concrete to conventional concrete - ScienceDirect, (n.d.). (Accessed 7 March 2022).
[131] Effect of Sodium Hydroxide Additive on Mechanical Properties and Durability of Self-Compacting Concrete with Sulfate Aggregates in Chloride Environment | SpringerLink, (n.d.). (Accessed 7 March 2022).
[132] Markssuel Teixeir,Marvilaab Afonso Rangel Garcezd Azevedo Leandro Barbosad Oliveirab Gustavode Castro Xavier Carlos Maurício Fontes Vieira, Mechanical, physical and durability properties of activated alkali cement based on blast furnace slag as a function of %Na2O - ScienceDirect, (n.d.). (Accessed 7 March 2022).
[133] M.T. Marvila, A.R.G. de Azevedo, P.R. de Matos, S.N. Monteiro, C.M.F. Vieira, Rheological and the fresh state properties of alkali-activated mortars by blast furnace slag, Materials 14 (2021) 2069, https://doi.org/10.3390/ma14082069.